Chemo-mechanical characterization and data-driven correlation analysis of rejuvenated bitumen via artificial neural network

Ren, Shisong; Khadijeh, Mahmoud; Assaf, Eli I.; Liu, Xueyan; Erkens, Sandra

DOI
10.1016/j.matdes.2025.114250

Publication date
2025

Document Version
Final published version

Published in
Materials and Design

Materials & Design 256 (2025) 114250

Contents lists available at ScienceDirect

Materials & Design

journal homepage: www.elsevier.com/locate/matdes

Chemo-mechanical characterization and data-driven correlation analysis of rejuvenated bitumen via artificial neural network

Shisong Ren [a,b,*], Mahmoud Khadijeh [a], Eli I. Assaf [a], Xueyan Liu [a], Sandra Erkens [a]

[a] Section of Pavement Engineering, Faculty of Civil Engineering & Geosciences, Delft University of Technology, the Netherlands
[b] Sustainable Pavement and Asphalt Research (SuPAR) group, Faculty of Applied Engineering, University of Antwerp, Belgium

ARTICLE INFO

Keywords:
Rejuvenation efficiency
Bitumen source
Rejuvenator type
Chemo-mechanical correlation
Artificial neural network

ABSTRACT

The chemo-mechanical properties of bitumen undergo significant alternations during aging and rejuvenation, posing challenges for accurately evaluating and enhancing rejuvenation efficiency in asphalt recycling. This study investigates how bitumen source, aging degree, rejuvenator type and dosage influence the chemical and rheological performance of rejuvenated bitumen. Comprehensive characterizations are performed using saturate, aromatic, resin, and asphaltene (SARA) fractionation, elemental analysis, gel permeation chromatography (GPC), and dynamic shear rheometer (DSR) tests. To elucidate chemo-rheological correlations, statistical techniques (Pearson correlation, analysis of variance (ANOVA), and Chi-square tests) are combined with artificial neural networks (ANN). Results indicate that the NB bitumen with more colloidal stability and less sulfur content exhibits the highest resistance to long-term aging. FB bitumen with 4.3 % sulfur achieves the best high-temperature deformation resistance with rutting failure temperature (RFT) higher than 80 °C, and TB bitumen exhibits the longest fatigue life. Rejuvenation using bio-oil is most effective on reducing relaxation time by up to 60 % and increasing creep compliance ($J_{nr3.2}$) by 1.7–2.5 times, depending on bitumen type. Rejuvenator dosage sensitivity for relaxation stress follows the trend: bio-oil < engine-oil < naphthenic-oil, while aromatic-oil shows variability depending on its source. Among the tested rejuvenators, bio-oil proves most effective, particularly for rejuvenating TB and FB bitumen. The ANN model demonstrates strong predictive performance for rheological properties, achieving R^2 values between 0.90 and 0.98, with the highest accuracy observed for relaxation indices, followed by fatigue and rutting properties.

1. Introduction

Asphalt concrete is one of the most commonly used materials in flexible pavements, with global production of asphalt mixtures for paving estimated to exceed one billion tons annually [1,2]. The practice of recycling by reusing reclaimed asphalt (RA) materials in pavement construction has gained prominence worldwide, driven by its environmental benefits, such as reducing CO_2 emissions and conserving natural resources, as well as economic advantages like cost savings, energy efficiency, and lower transportation costs [3–5]. The growing demand for sustainable solutions has led to the widespread adoption of RA recycling techniques, fostering a circular economy in the construction industry [6].

However, incorporating RA materials into asphalt mixtures can raise durability concerns, such as increased moisture susceptibility and diminished resistance to cracking and fatigue, due to the aged and stiff bitumen present in RA materials [7,8]. As a result, the common practice is to limit the RA content in new asphalt pavements to ensure satisfactory engineering performance [9]. To increase the RA content beyond 30 %, rejuvenators—or recycling agents—are employed to reactivate and enhance the cohesive and adhesive properties of the aged bitumen [10,11].

Rejuvenators can be sourced from a variety of materials, including plant oils, waste-derived oils, engineered products, and both traditional and non-traditional refinery base oils [12,13]. It has been proved that the rejuvenation efficiency of different rejuvenators is strongly dependent on various influence factors, such as bitumen source (type) [14], aging level of bitumen [15], rejuvenator type [16] and dosage [17]. Additionally, the bitumen source also affects the aging kinetics and mechanism of bitumen, further influencing the service life and recycling efficiency of asphalt pavement [18,19]. Similarly, it was reported that the rheological properties of modified asphalt were affected by different

* Corresponding author at: Section of Pavement Engineering, Faculty of Civil Engineering & Geosciences, Delft University of Technology, the Netherlands.
E-mail address: Shisong.Ren@uantwerpen.be (S. Ren).

https://doi.org/10.1016/j.matdes.2025.114250
Received 25 April 2025; Received in revised form 5 June 2025; Accepted 15 June 2025
Available online 17 June 2025

Table 1
Basic properties of three virgin bitumen.

Items	TB	FB	NB	Test standard
25 °C Penetration (0.1 mm)	91	89	101	ASTM D5 [28]
Softening point (°C)	48.0	47.6	46.2	ASTM D36 [29]
Complex modulus G* (kPa)*	2.4	2.1	1.6	AASHTO M320 [30]
Phase angle δ (°)*	84.5	85.1	86.2	

* G* and δ values are measured at 60 °C and 1.6 Hz.

bitumen sources [20], and the magnitude of the changes on bitumen performance during the aging was dependent on the bitumen type and evaluation indicators [21]. However, other study mentioned that changing the type of bitumen showed no significant effect on the healing capacity of asphalt mix. The complex chemical components in rejuvenated bitumen lead to a big challenging to get a uniform conclusion on rejuvenation efficiency evaluation. On the other hand, the chemo-mechanical correlations of virgin, aged, and rejuvenated bitumen were elucidated [22,23], but it is difficult to predict the rheological properties of rejuvenated bitumen based on chemical characteristics.

Machine learning offers a powerful approach to bridging the gap between the chemical and rheological properties of bitumen. By analysing vast datasets, machine learning models can identify complex patterns and relationships that traditional methods might overlook [24]. This enables more accurate predictions of how chemical composition influences the rheological behavior of bitumen, such as its viscosity, elasticity, and overall performance under varying conditions. Salehi et al. [25] adopted four ensemble machine learning models, Random Forest (RF), eXtreme Gradient Boosting (XGBoost), Categorical Boosting (CatBoost), and Light Gradient-Boosting Machine (LightGBM), to predict rheological properties of recycled plastic modified bitumen. It was concluded that the CatBoost method showed the best prediction efficiency on both complex shear modulus and phase angle. Shan et al. [26] found the Support Vector Machine (SVM) model was better to predict the viscoelastic property of bitumen with input parameters of chemical characteristics (element compositions and molecular vibrations) than relevance vector machine (RVM) and random forest (RF). Similarly, Asadi and Hajj [27] adopted tree-based ensemble bagging and boosting models to precisely predict the elastic recovery of bitumen from the Multiple Shear Creep and Recovery (MSCR) test results. These successful cases verify the application potential of machine learning methods on chemo-mechanics performance prediction and correlations of bitumen. Nevertheless, there is limited study on the chemo-rheological correlations of rejuvenated bitumen for effective selection and optimization of rejuvenator.

To this end, this study aims to investigate the chemical and rheological behaviour of rejuvenated bitumen as influenced by variable bitumen sources, rejuvenator types and dosages, and to further explore the underlying chemo-mechanical relationships. A comprehensive analysis is first performed to evaluate how these factors affect the chemical properties (SARA fractions, element compositions, molecular weight distribution) and rheological properties (high-temperature rutting resistance, low-temperature relaxation capacity, and fatigue). Subsequently, statistical and machine learning approaches are employed to predict and interpret the chemo-mechanical correlations in rejuvenated bitumen.

2. Materials and measurements

2.1. Materials

In this study, three bitumen with the same PEN70/100 but from different sources were used, coded as TB, FB, and NB. Their basic properties are listed in Table 1. Meanwhile, three petroleum-based rejuvenators and one bio-based rejuvenator were selected to regenerate the chemo-rheological properties of aged bitumen, which are engine-oil (EO), naphthenic-oil (NO), aromatic-oil (AO), and bio-oil (BO) [15,16]. Table 2 summarizes the chemical and physical properties of all rejuvenators.

Table 2
Physical and chemical properties of different rejuvenators.

Items	BO	EO	NO	AO	Test standard
25 °C density ($g{\cdot}cm^{-3}$)	0.911	0.833	0.875	0.994	EN 15,326 [31]
60 °C density ($g{\cdot}cm^{-3}$)	0.899	0.814	0.852	0.978	
25 °C Viscosity (cP)	50	60	130	63,100	AASHTO T316 [32]
Color	Pale yellow	Brown	Transparent	Dark-brown	
Flash point	265–305	>225	>230	>210	ASTM D93 [33]
N% (wt%)	0.15	0.23	0.12	0.55	ASTM D7343 [34]
C% (wt%)	76.47	85.16	86.24	88.01	
H% (wt%)	11.96	14.36	13.62	10.56	
S% (wt%)	0.06	0.13	0.10	0.48	
O% (wt%)	11.36	0.12	1.90	0.40	
M_n ($g{\cdot}mol^{-1}$)	286.4	316.5	357.1	410.0	ASTM UOP676 [35]

2.2. Aging procedures

Three types of fresh bitumen were subjected to Thin-Film Oven Test (TFOT) and Pressure Aging Vessel (PAV) test to simulate short-term and long-term aging. In the TFOT test, bitumen samples were aged at 163 °C for 5 h. The short-term aged bitumen was then transferred to the PAV test, conducted at 100 °C under a pressure of 2.1 MPa. The long-term aging durations were set at 20, 40 and 80 h. The corresponding abbreviations for virgin, short-term aged, and long-term aged bitumen are VB, SAB, LAB20, LAB40, and LAB80, respectively.

2.3. Preparation of rejuvenated bitumen

To ensure sufficient flowability, the aged bitumen was first preheated in an oven at 150 °C for 30 min. The rejuvenators (BO, EO, NO, and AO) were added at dosages of 5 %, 10 %, and 15 % by weight of aged bitumen, based on our previous optimization study [36]. The blending was conducted using a high-shear mixer at 150 °C for 10 min at a stirring speed of 1000 rpm to ensure uniform dispersion of the rejuvenator within the aged bitumen. Throughout the process, the temperature was carefully monitored and maintained using a temperature-controlled heating plate. The blend was visually inspected to confirm the absence of phase separation, indicating the formation of homogeneous rejuvenated bitumen.

2.4. Chemical characterization methods

2.4.1. Thin-layer chromatography with flame ionization detection (TLC-FID)

In this study, the mass fraction of the saturate, aromatic, resin, and asphaltene in different virgin and aged bitumen were measured by the TLC-FID method [37]. The flow rate of air and hydrogen was set as 2 $l{\cdot}min^{-1}$ and 160 $l{\cdot}min^{-1}$, respectively. The bitumen/toluene solution was firstly prepared by dissolving around 0.1 g bitumen in 10 ml toluene, and chromatography separated with a silica chrome rod. The saturate fraction was detected with the chromatographical separation process in n-heptane, while the aromatic and resin fractions were measured in toluene/n-heptane (80:20) and dichloromethane/methanol (95:5) solvents. Lastly, the asphaltene concentration was remained at the sampling spot.

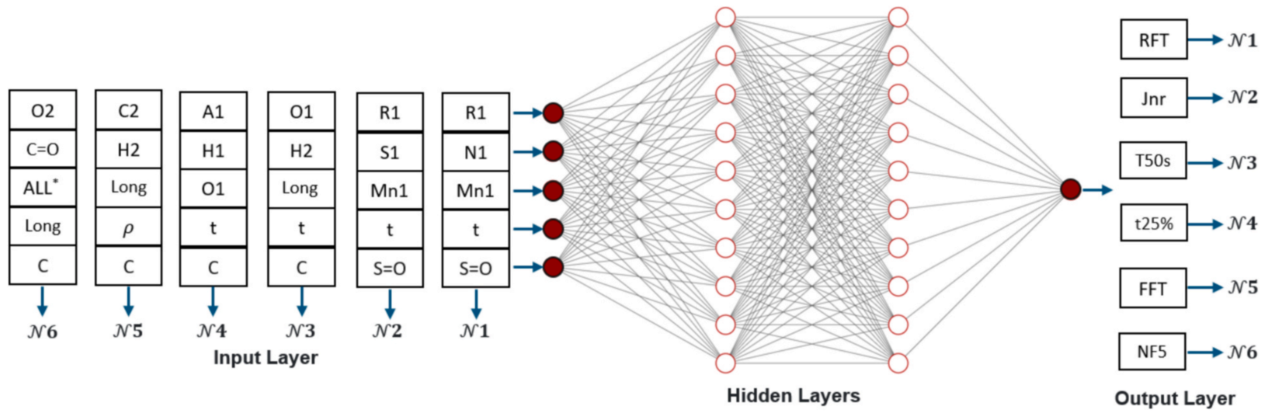

Fig. 1. Artificail Netural Network (ANN) modelling on chemo-mechanics correlations: rutting failure temperature (RFT), creep compliance (J_{nr}), shear stress at 50 s ($T50_S$), relaxation time at 25 % stress ($t_{25\%}$), fatigue failure temperature (FFT), fatigue life at 5 % stain (NF5).

2.4.2. Elemental analysis

The elemental components of various virgin and aged bitumen were measured using an elemental analyser [37]. First, the element analysis on one reference substance (sulfanilamide) was performed to do calibration work. Afterward, 5–10 mg bitumen specimen was encased in a tin capsule to measure the mass percent of the elements: carbon (C), nitrogen (N), oxygen (O), hydrogen (H), and sulfur (S).

2.4.3. Gel permeation chromatography (GPC)

The variation of molecular weight distribution for three bitumen during short-term and long-term aging processes was monitored by the GPC test [37]. The mobile solvent was the tetrahydrofuran (THF) with a flow rate of 1 ml·min^{-1}. About 0.05 g bitumen was first dissolved in THF solvent (10 ml) at room temperature, and the solution was filtered through a syringe filter before injection. For all chemical tests, three repetition tests were conducted for each sample to ensure the accuracy of the results.

2.5. Rheological measurements

2.5.1. Temperature sweep test

The dynamic shear rheometer (DSR) was employed to monitor the variations of complex modulus (G*) and phase angle (δ) of bitumen as a function of temperature, increasing from 0℃ to 70℃ with a fixed frequency of 10 rad/s and an interval of 10℃. The rutting failure temperature (RFT) was calculated when the rutting parameter (G*/sinδ) of fresh bitumen was equal to 1.0 kPa. Meanwhile, the fatigue failure temperature (FFT) was determined when the fatigue parameter (G*sinδ) was equal to 5000 kPa [37].

2.5.2. Multiple stress creep and recovery (MSCR) test

It was observed that the non-recoverable creep compliance ($J_{nr3.2}$) could distinguish and evaluate the rejuvenation efficiency of different rejuvenators [38]. The $J_{nr3.2}$ values of all bitumen were measured through MSCR test at 58℃ and stress level of 3.2 kPa. The MSCR test contains ten cycles, and each cycle is composed on 1 s creep and 9 s recovery.

2.5.3. Relaxation test

The relaxation test was conducted with DSR at 0℃ and a fixed strain level of 1 %. The sample was subjected the increasing strain loading first from 0 to 0.1 s, followed by a constant-strain loading from 0.1 to 100 s. Based on previous work [39], two key relaxation parameters, residue shear stress at 50 s (τ_{50s}) and relaxation time at 25 % residue stress ($t_{25\%}$).

2.5.4. Linear amplitude sweep (LAS) test

The LAS test was performed at 20℃ and 10 Hz with the applied strain increasing from 0.1 % to 30 % linearly. The total test time and loading cycle number are 310 s and 3100 cycles, respectively. The simplified viscoelastic continuum damage (S-VECD) modelling was used to propose several fatigue parameters for assessing the effects of bitumen type, aging level, rejuvenator type/dosage on the fatigue life (N_{f5}) of bitumen. Meanwhile, the elastic modulus (E) and strain ($\mathcal{E}_{sr}$) were derived from the τ-γ curves [40]. For all rheological tests, each sample underwent triplicate testing to ensure result reliability.

2.6. Statistical analysis and machine learning methods

In this study, the correlation potentials between different chemical and rheological parameters of all rejuvenated bitumen are explored using different statistical analysis methods: Pearson correlation, analysis of variance (ANOVA), and Chi-square methods. The Pearson correlation coefficient is the most widely used measure of the linear relationship between two variables. Its value ranges from + 1 to −1, where + 1 indicates a perfect positive linear correlation, 0 indicates no linear correlation, and −1 indicates a perfect negative linear correlation [41,42]. The ANOVA is a statistical method used to compare the means of three or more groups to determine if there are significant differences between them. By analysing the variation within and between groups, ANOVA helps identify whether any of the group means differ significantly. The detailed calculations can be found in previous work [43]. The Chi-square test is a non-parametric method commonly-used to examine the independence between variables and to test the goodness-of-fit, determining how well the observed data distribution matches the expected distribution. It is particularly useful to analysing categorical data by assessing significance through the chi-squared statistic. This statistic is derived from the sum of squares of independent variables, calculated as the weighted sum of squared differences between observed and expected frequencies [44]. To evaluate whether the differences between these frequencies are significant, the following equation can be applied:

$$\chi^2 = \sum_{i=1}^{n} \frac{(O_i - E_i)^2}{E_i} \tag{1}$$

where O_i and E_i is the observed and expected frequency value, respectively.

To predict the key rheological properties of rejuvenated bitumen using various chemical input parameters, an Artificial Neural Network (ANN) modelling approach is employed. ANN is a machine learning algorithm inspired by the structure and function of human neurons, simulating the way the brain processes and learns from data. In this study, six independent neural network models were developed to predict a specific property of bituminous materials. These models use six input

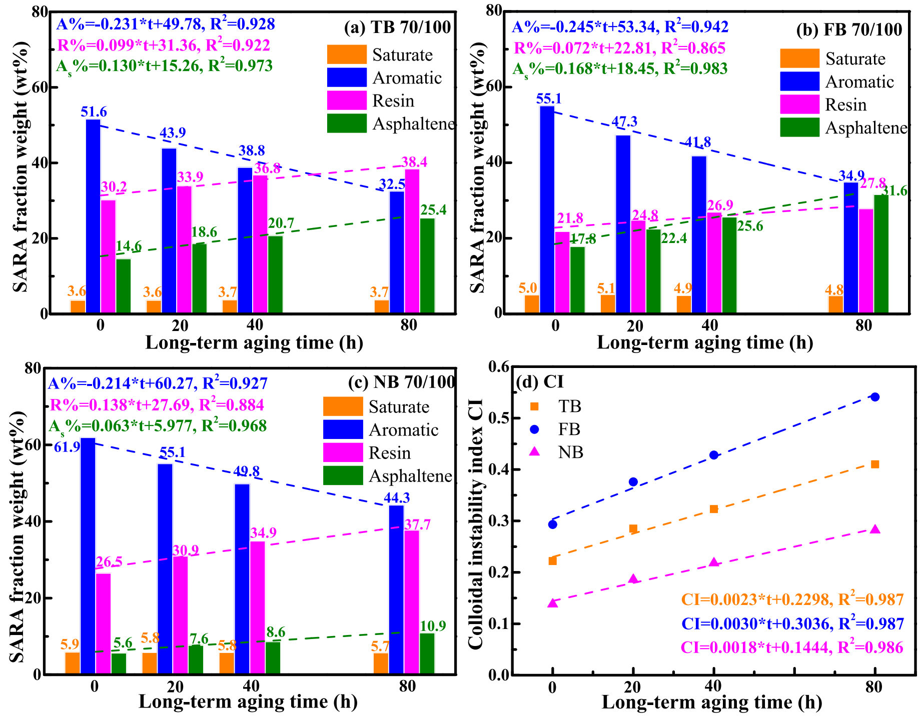

Fig. 2. Chemical component variations of different bitumen during long-term aging.

features to predict a single output variable, enabling precise estimation of individual bitumen characteristics. This approach allows the models to capture the distinct relationships between input parameters and the target property, thereby improving prediction accuracy and reliability. The modelling procedure consists of four steps, as illustrated in Fig. 1.

Different steps are involved as: (i) Data Preparation: Features (inputs) and targets (outputs) were normalized using MinMaxScaler to ensure consistent scaling [45]. The data was split into training (80 %) and testing (20 %) sets for each model. (ii) Model Architecture: Each of the six neural networks features an input layer with six neurons, representing the six physicochemical properties of asphalt mixtures. The architecture includes two hidden layers, each comprising 128 neurons with Rectified Linear Unit (ReLU) activation functions [46]. The output layer consists of a single neuron with a linear activation function to predict the specific target property. To prevent overfitting, a dropout rate of 0.2 was applied after each hidden layer. (iii) Training Process: Each model was trained independently using the Adam optimizer, with Mean Squared Error (MSE) as the loss function. Training was conducted over a maximum of 1000 epochs with a batch size of 32. Early stopping was implemented with a patience of 20 epochs to prevent overfitting. (iv) Model Evaluation: The performance of each model was assessed using multiple metrics: MSE for both training and testing sets, R-squared (R^2) scores to quantify the proportion of variance explained by each model, visual analysis of predicted vs. true values for both training and testing datasets.

3. Results and discussion

3.1. Chemo-mechanical behaviors of aged bitumen

3.1.1. SARA fractions

The SARA fractions of three bitumen and various aged bitumen under different long-term aging time are displayed in Fig. 2. Regardless of bitumen type, the saturate dosage keeps almost stable during long-term aging, which significantly declines the aromatic concentration and increases both resin and asphaltene fractions. Meanwhile, the aromatic, resin, and asphaltene present the linear variation trends as a function of long-term aging time. However, their variation levels depend on the bitumen type. Regarding the aromatic fraction, the NB bitumen shows the highest concentration at the virgin state, followed by the FB and TB bitumen. Meanwhile, the long-aging time exhibits the largest reduction effect on the aromatic percentage of FB bitumen, followed by the TB and NB ones.

The increasing rate of resin fraction in NB bitumen is higher than the TB and FB bitumen, while the increasing rate of asphaltene is the lowest. It shows that compared to other two bitumen, the NB bitumen is more indicated to generate more resin fractions during the long-term aging process, which is related to its high aromatic and low asphaltene fractions. From the SARA ratio, the long-term aging resistance of NB is better than the others, and its asphaltene percentage (10.9 %) after 80-hours long-term aging is still much lower than TB (25.4 %) and FB (31.6 %).

The TB and NB bitumen show the similar long-term aging behaviors, but the variation rates are not the same. The reduction rate of aromatic in FB bitumen is slightly larger that TB one, but the resin generation rate of the latter one is higher. Additionally, the increasing rate of asphaltene in FB bitumen is faster than the TB one, indicating that it is easier for FB bitumen to consume the aromatic/resin fractions to the asphaltene than the TB bitumen. Thus, the long-term aging resistance of FB bitumen seems to be a little worse than the TB one. The colloidal instability index CI results, calculated as Eq. (2), are plotted in Fig. 2(d). It is noted that a higher CI value indicates lower colloidal stability of bitumen.

$$CI = \frac{A_s\% + S\%}{A\% + R\%} \tag{2}$$

where $A_s\%$ and S% represents the asphaltene and saturate dosage, and the A% and R% are the aromatic and resin concentration.

As the aging time prolongs, the CI values of all bitumen tend to increase increasingly. It means that the long-term aging deteriorates the colloidal stability of bitumen. Similarly, the aging susceptibility of CI parameter relies on the bitumen type. Based on the equation slope, the same finding is observed that the FB bitumen shows the highest aging susceptibility, followed by TB and NB bitumen. Meanwhile, the order of CI values is FB > TB > NB, regardless of the long-term aging levels. It indicates that the FB bitumen will show the worst colloidal stability,

Table 3
Element components of different bitumen with variable long-term aging time.

Bitumen source	Aging level	C%	N%	H%	O%	S%	H/C
TB 70/100	VB	84.06	0.90	10.90	0.62	3.52	1.556
	SAB	83.72	0.91	10.86	1.00	3.51	1.557
	LAB20	83.26	0.92	10.75	1.58	3.49	1.549
	LAB40	83.02	0.89	10.44	2.11	3.53	1.509
	LAB80	82.14	0.91	10.10	3.31	3.54	1.476
FB 70/100	Fresh	82.53	0.60	10.36	2.22	4.30	1.506
	SAB	82.21	0.61	10.32	2.59	4.29	1.506
	LAB20	81.78	0.61	10.21	3.13	4.26	1.498
	LAB40	81.45	0.59	9.92	3.72	4.31	1.462
	LAB80	80.66	0.61	9.56	4.85	4.33	1.422
NB 70/100	Fresh	85.56	0.66	10.50	2.00	1.28	1.473
	SAB	85.20	0.67	10.46	2.39	1.28	1.473
	LAB20	84.72	0.67	10.35	2.99	1.27	1.466
	LAB40	84.47	0.65	10.07	3.53	1.29	1.431
	LAB80	83.70	0.67	9.77	4.58	1.29	1.401

while the NB one has the best. The correlations between SARA fractions and rheological parameters will be explored in the following section.

3.1.2. Element analysis

The element compositions of these three bitumen before and after aging are listed in Table 3. The elemental components of different bitumen and their sensitivity to long-term aging are different. The TB and NB bitumen show a higher C% than the FB bitumen, and the TB bitumen has the highest N%. However, the order of O% content in fresh bitumen is FB > NB > TB. Regarding the S% dosage, the FB shows the highest value, followed by TB and NB bitumen. There is no big difference in H% of different bitumen, while the TB bitumen shows the highest H/C ratio, followed by FB and NB.

Regardless of bitumen type, the long-term aging leads to a reduction of C%, H%, but an increase in O%. It is related to the oxidation reaction of bitumen molecules and generation of oxygen-containing functional groups, such as sulfoxide and carbonyl [47]. It is observed that the aging level has no influences on the order of O% content in three bitumen. Meanwhile, the high S% dosage in FB bitumen contributes to its largest O% after aging due to the formation of more S=O groups. Lastly, the N% and S% values of all bitumen are not affected by long-term aging process.

3.1.3. Molecular weight distribution

Apart from the variation of element component and functional group distribution, the impacts of bitumen type and long-term aging on the weight-average molecular weight (M_w), number-average molecular weight (M_n), and polydispersity index (D) are displayed in Fig. 3. The standard GPC curves of TB bitumen with variable long-term aging levels are plotted in Fig. 3(a). As the aging degree extends, the heavy-weight molecule ratio increases gradually, which agrees the SARA results. The TB bitumen shows the higher M_w and M_n values than the FB and NB bitumen. The FB bitumen has a slightly higher M_w than the NB bitumen, while the former presents the lowest M_n value. The elevated M_w and M_n values observed in TB bitumen are likely attributed to the presence of heavier and structurally more complex molecules with its maltene phase, particularly among the aromatic and resin fractions [48]. These components can significantly influence molecular weight averages, even when the overall asphaltene content is relatively low. In contrast, although FB bitumen exhibits a higher asphaltene content and a correspondingly high colloidal instability index (CI), this does not necessarily translate into higher M_w and M_n. This may be due to oxidative degradation or molecular fragmentation of the maltene components during processing, which offsets the contribution of asphaltenes to the overall molecular weight distribution [49,50]. Both M_w and M_n indices of all bitumen linearly increase as the long-term aging level rising, related to the increment of heavy-weight molecules (resin and asphaltene) and

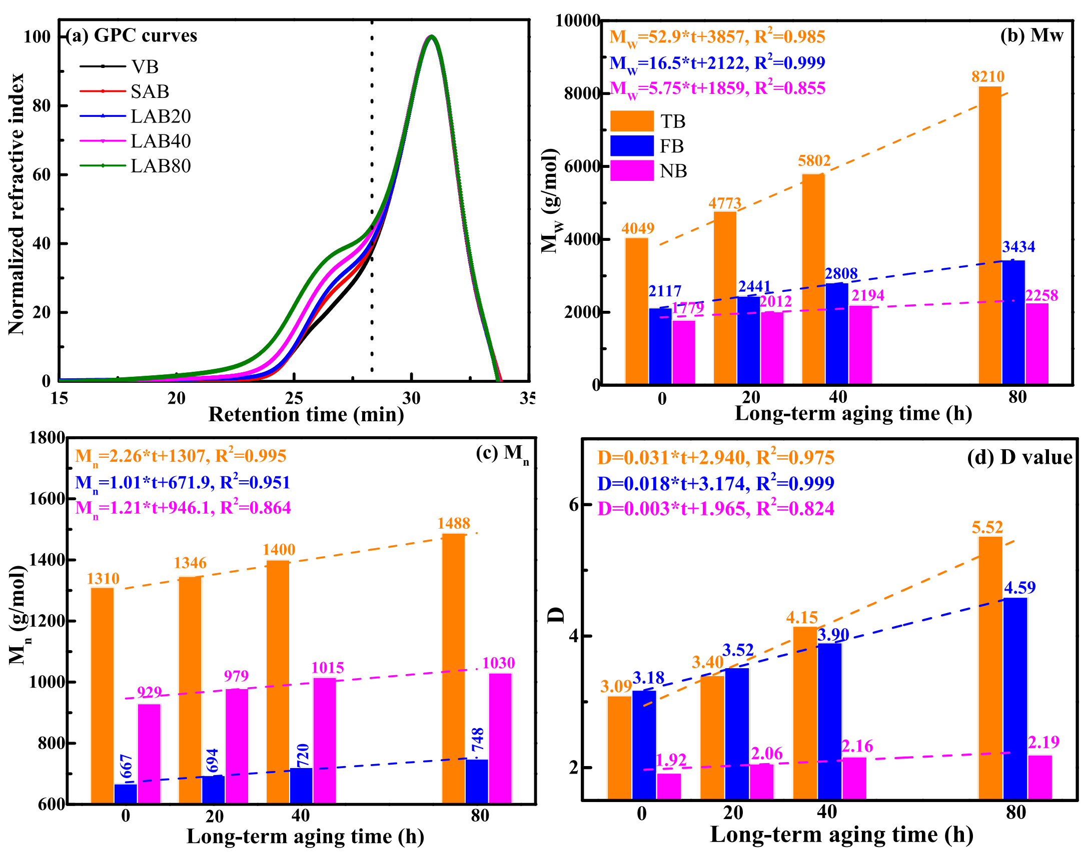

Fig. 3. Molecular weight distribution change of different bitumen during long-term aging.

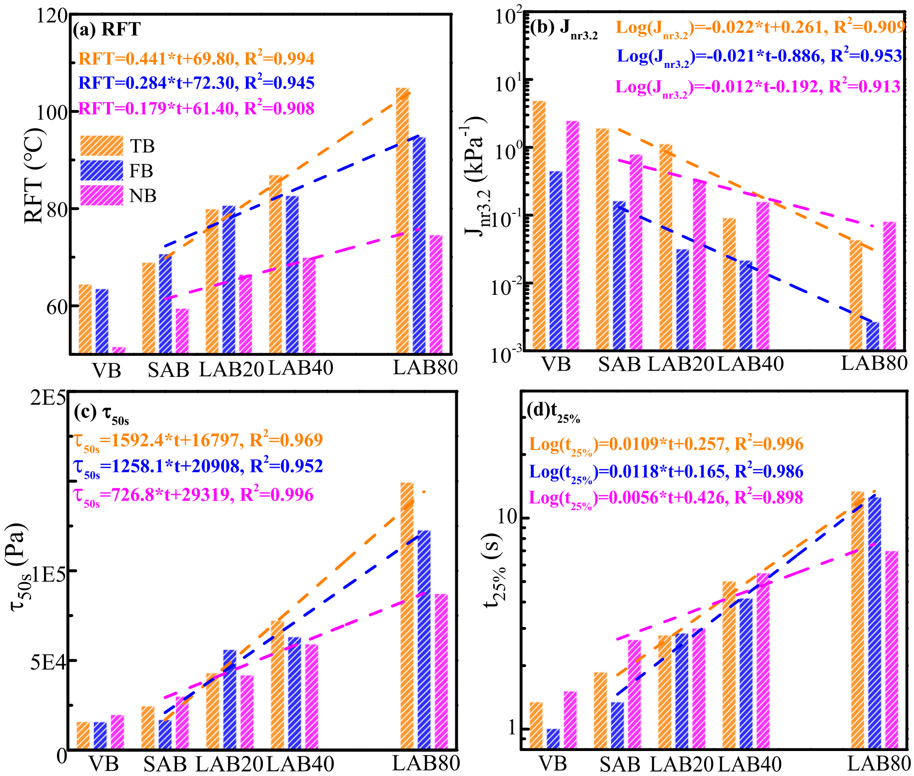

Fig. 4. Effect of aging level on the high-and-low temperature properties of different bitumen.

reduction of light-weight molecules (aromatic). In addition, the aging susceptibility of M_w and M_n indices depends on the bitumen type. The increasing rate of M_w value of TB bitumen is the highest, followed by FB and NB. It indicates that the aging resistance of TB bitumen is the worst based on both M_w and M_n results. The variation trend of D values is shown in Fig. 3(d). Both TB and FB bitumen show the higher D values than the NB, indicating that the NB bitumen is mainly composed of light-weight molecules. Moreover, all D values tend to increase linearly during the long-term aging process, showing that more heavy-weight molecules are generated. Based on the absolute slope values of D-t correlation equations, the D value of TB bitumen changes a lot, followed by the FB bitumen, while the NB bitumen presents the lowest aging susceptibility.

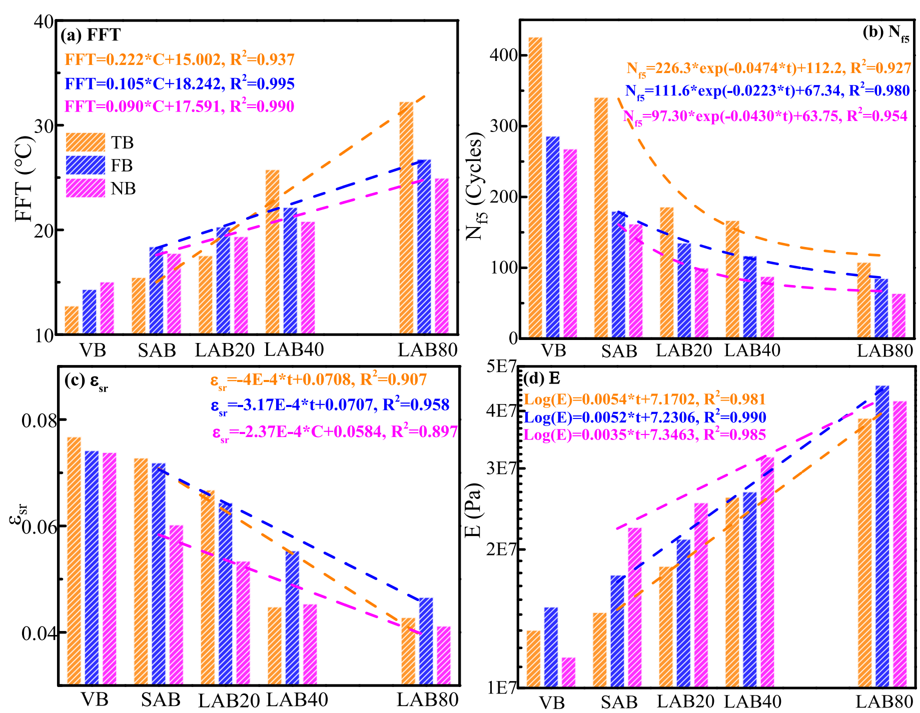

Fig. 5. Effect of aging level on the fatigue properties of different bitumen.

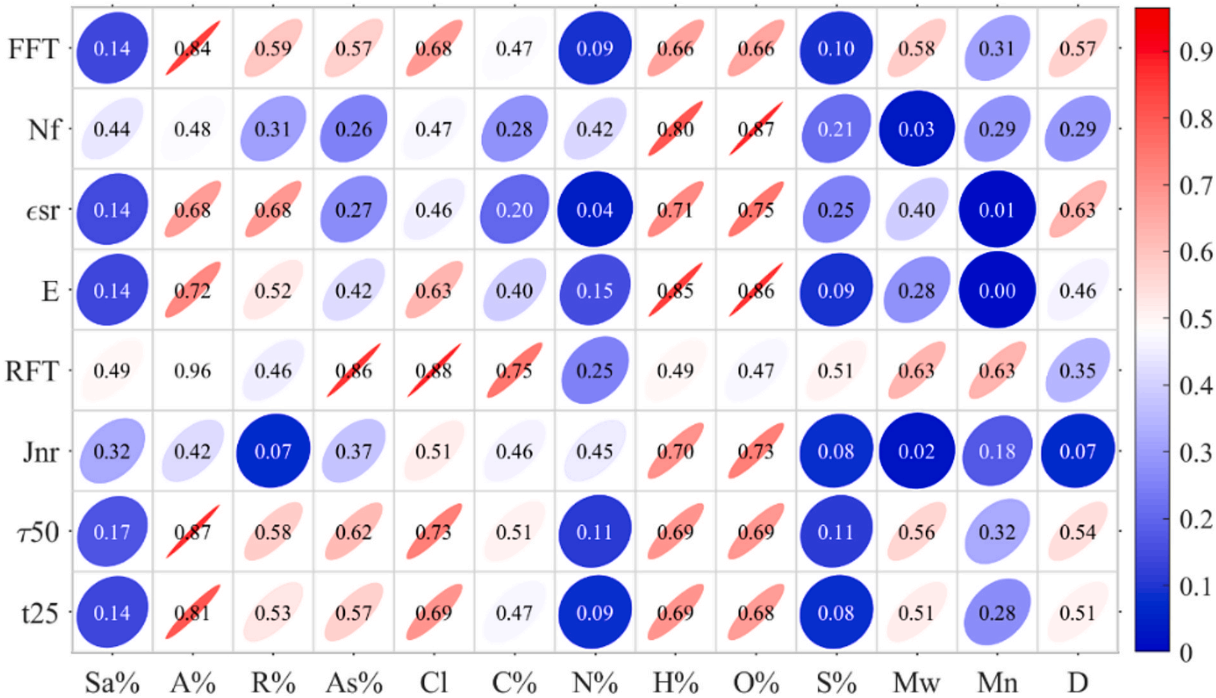

Fig. 6. Absolute correlation level between chemical and rheological properties.

3.1.4. High-and-low temperature properties

Two parameters, rutting failure temperature (RFT) and creep compliance ($J_{nr3.2}$), are adopted to assess the effects of long-term aging on the high-temperature performance of various bitumen. The results are shown in Fig. 4(a) and (b). For all bitumen types, the long-term aging leads to higher RFT and lower $J_{nr3.2}$ values, which is related to the enhanced elastic and rutting resistance performance of bitumen. Meanwhile, their variation trends are linear and depend on the bitumen type. Similar to molecular weight result, the increasing level in RFT and decreasing degree in $J_{nr3.2}$ of the TB bitumen is the most significant, followed by the FB and NB. When the aging level is the same, the RFT ranking is TB > FB > NB, while the $J_{nr3.2}$ sequence is TB > NB > FB. It

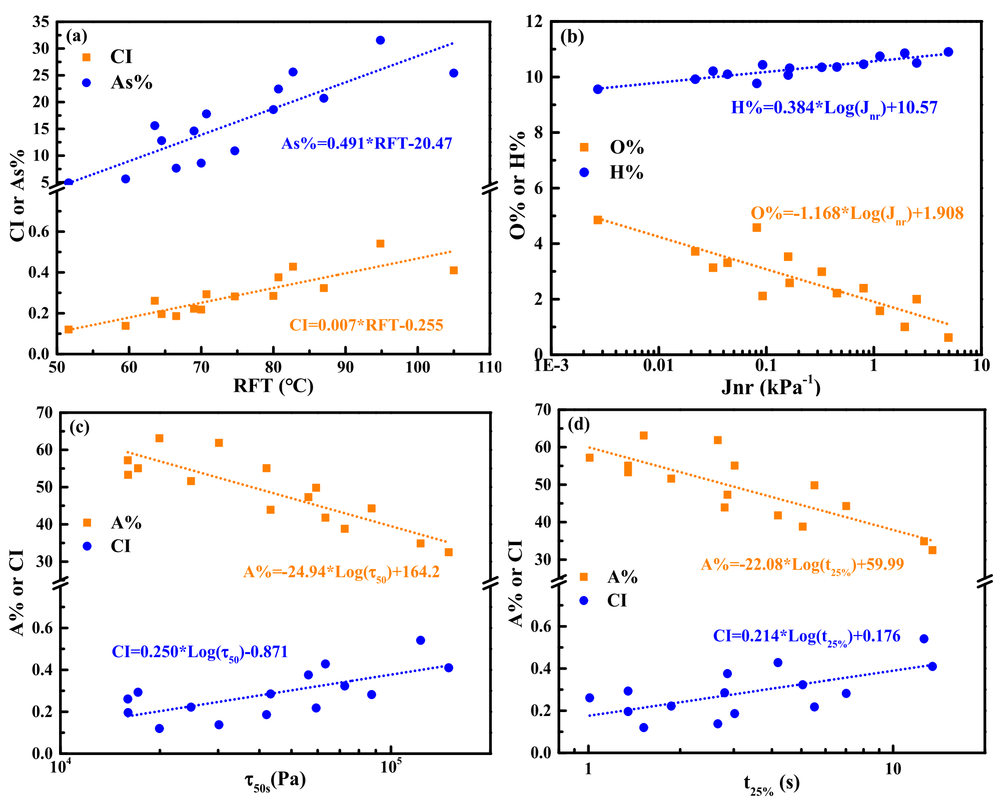

Fig. 7. Correlation curves between high-and-low temperature and chemical indices.

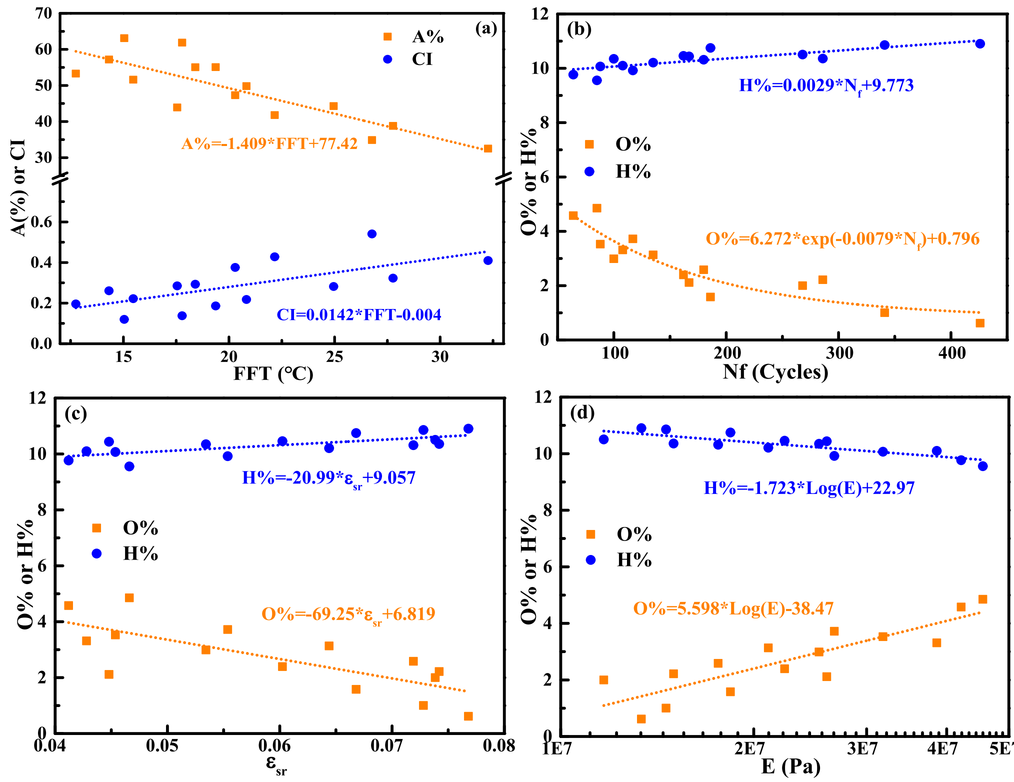

Fig. 8. Correlation curves between fatigue indices and chemical characteristics.

means that the TB bitumen displays the best rutting resistance but the worst aging resistance.

Fig. 4 (c) and (d) illustrate the low-temperature relaxation properties of different virgin and aged bitumen with two parameters: shear stress at 50 s (τ_{50s}) and relaxation time with 25 % residue stress ($t_{25\%}$). Regardless of bitumen type, both τ_{50s} and Log($t_{25\%}$) values show a linearly-increasing trend. It means that long-term aging deteriorates the low-temperature performance and increases the cracking potential of bitumen. The TB bitumen shows higher τ_{50s} and $t_{25\%}$ values than the FB and NB bitumen, implying that the TB bitumen present the worst low-temperature performance. Although the NB bitumen at fresh and short-term aged states shows the worse relaxation capacity, both τ_{50s} and $t_{25\%}$ values of LAB80 NB-bitumen are the lowest, showing that the NB bitumen presents the best low-temperature performance after long-term aging process because of the strongest aging resistance. Overall, high maltene fraction and low asphaltene dosage in NB bitumen contribute to its superior relaxation and anti-aging properties.

3.1.5. *Fatigue resistance*

Fig. 5 displays the fatigue indices of these three bitumen under variable aging conditions. Regardless of bitumen source, as the aging degree prolongs, the fatigue failure temperature (FFT) and elastic modulus (E) values increases linearly, while the fatigue life (N_{f5}) and ε_{sr} show the decreasing trend [37]. However, the bitumen type distinctly affects the fatigue properties, related to the aging level. Based on the FFT results, the fatigue resistance of TB bitumen with fresh and short-term aged states is better than the FB and NB bitumen, while its poor aging resistance leads to a significant deterioration in its fatigue performance. Additionally, the FB bitumen always shows a higher FFT value than the NB, indicating that the latter displays a better fatigue performance. Nevertheless, a converse finding is observed based on the N_{f5} results shown in Fig. 5(b). For all aging levels, the ranking of fatigue life for three bitumen is TB > FB > NB. The reason for the difference in findings may be related to the difference in loading ways. The FFT parameter is determined in a viscoelastic region, while the N_{f5} is derived from the LAS shear cracking test. Thus, the FFT index fails to assess the effects of bitumen type on the fatigue performance under variable aging degrees. It is observed that the FB bitumen shows the highest ε_{sr} values, followed by the TB and NB, while the order of E values follows TB < FB < NB. It further implies that the NB bitumen shows the worse fatigue life than the FB and TB.

3.1.6. *Chemo-mechanical correlation of aged bitumen*

It was observed that the long-term aging and bitumen type both affected chemical and rheological properties of bitumen. Is there any chemo-mechanical correlation working for all bitumen with variable aging level and bitumen type? The Pearson correlations between different chemical and rheological parameters were evaluated and the absolute correlation values are illustrated in Fig. 6. It is noted that as the correlation level increases, the ellipse becomes smaller in area and shifts in color from blue to red. Regarding the high-temperature performance, the RFT index shows strong correlations with colloidal instability index (0.88) and asphaltene dosage (0.86), while the J_{nr} correlates well with O% (0.73) and H% (0.70). Additionally, both relaxation parameters (τ_{50} and $t_{25\%}$) present high correlation efficient with aromatic dosage (A%) and CI index. It is interesting to note that the FFT index also has close connections with A% (0.84) and CI indicators, while other fatigue parameters (N_f, ε_{sr}, and E) link well to O% and H%.

The correlation curves between chemical indices and high-and-low temperature rheological parameters are plotted in Fig. 7. As the RFT increases, both CI and A_s% values of bitumen rise linearly, while the J_{nr} shows linear increasing and decreasing correlation with H% and O%, respectively. Thus, the high-temperature performance of fresh and aged bitumen from different sources can be predicted from chemical results. Meanwhile, the bitumen with higher CI, A_s%, O% values will present the better high-temperature deformation resistance, while the H% value has the opposite effect. Similarly, with the $\tau_{50\%}$ or $t_{25\%}$ rises, the CI parameter of bitumen increases and the A% value decreases linearly. It means that the bitumen with a higher aromatic dosage will show the faster relaxation capacity, while the CI parameter works conversely. It is

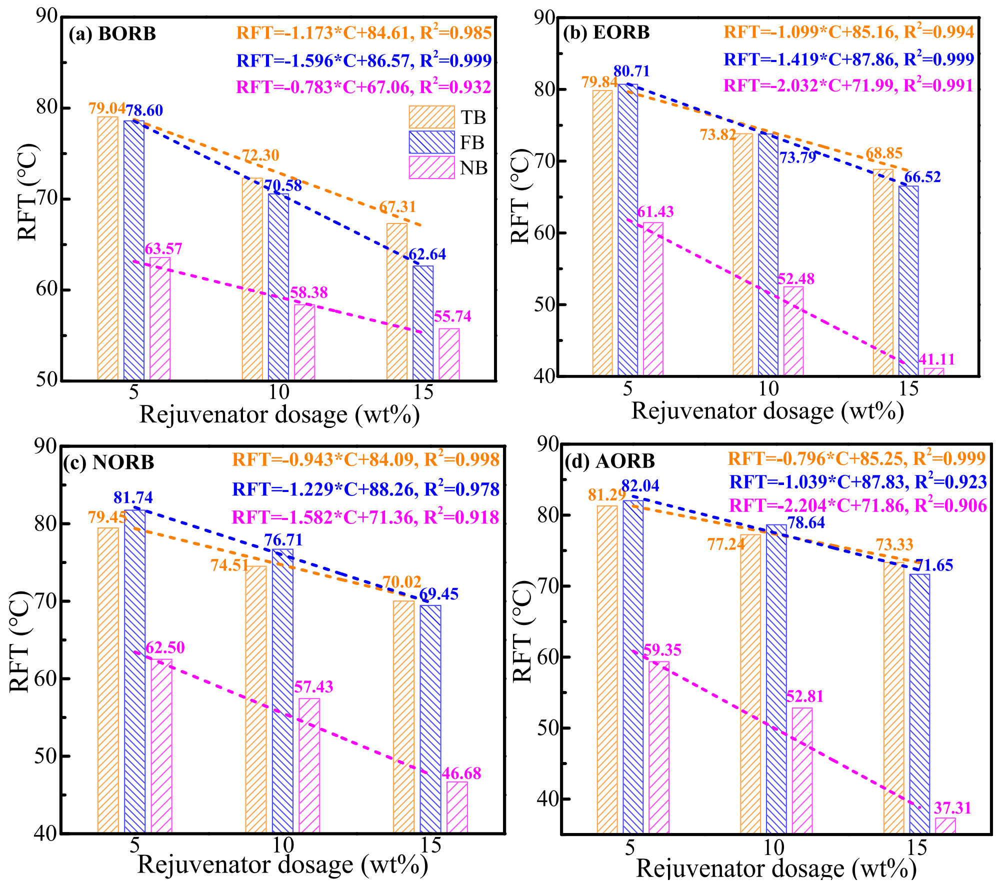

Fig. 9. Effect of bitumen type on the RFT values of rejuvenated bitumen.

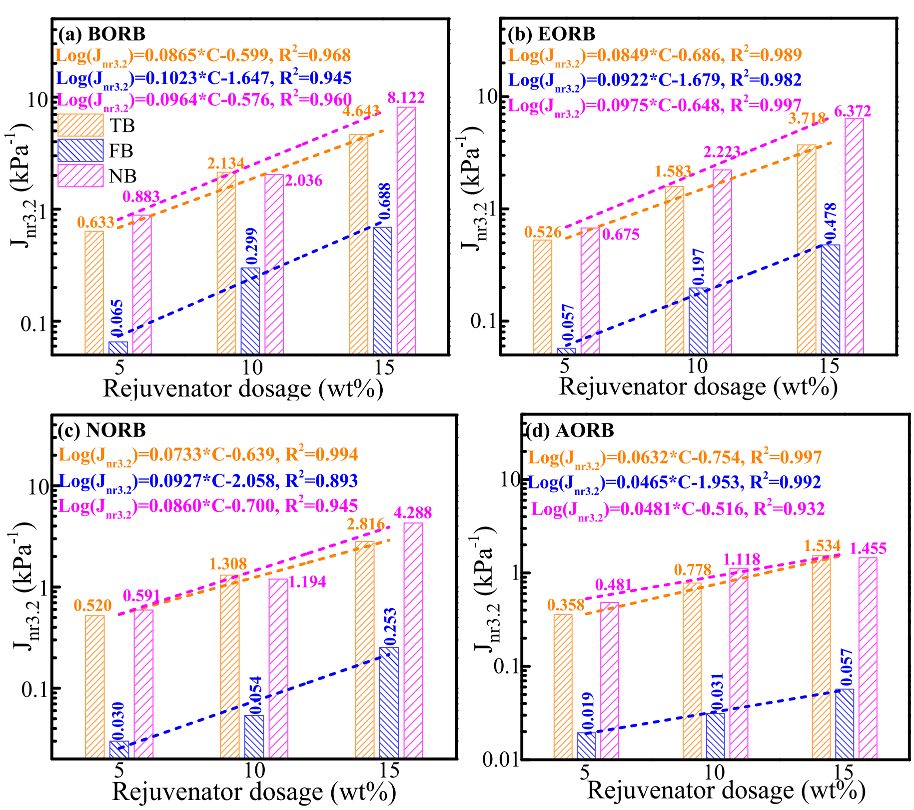

Fig. 10. Effect of bitumen type on the $J_{nr3.2}$ values of rejuvenated bitumen.

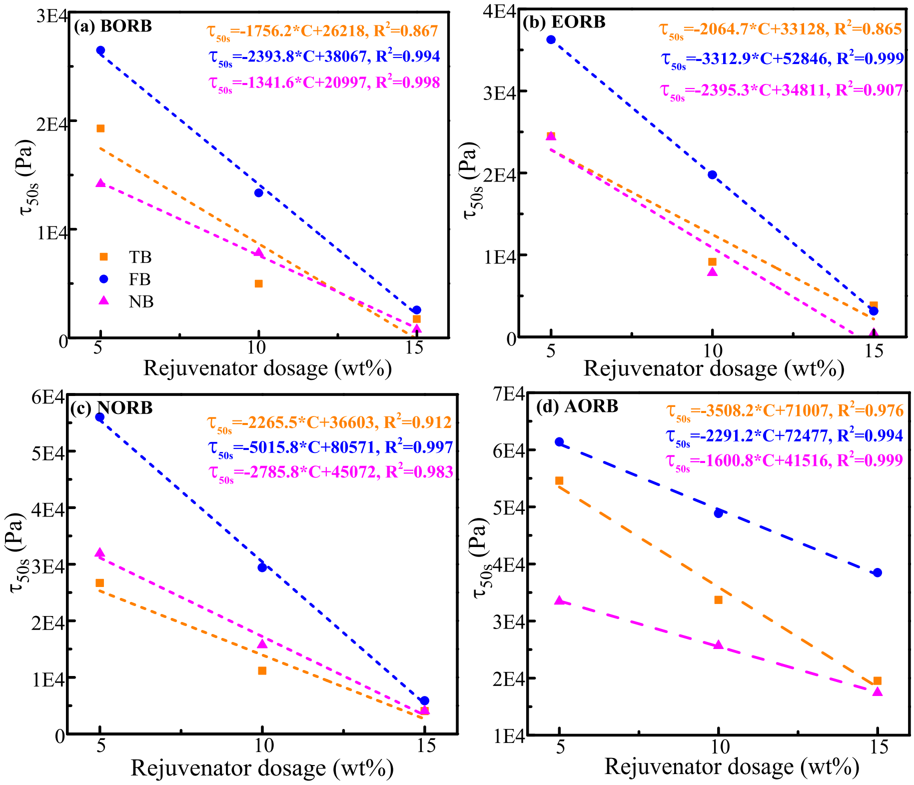

Fig. 11. Effect of bitumen type on the τ_{50s} values of rejuvenated bitumen.

interesting to mention that the CI index can correlate both with high-and-low temperature performance of bitumen.

Fig. 8 displays the potential connections between several chemical characteristics (A%, CI, O%, and H%) and fatigue parameters (FFT, N_f, ε_{sr}, and E) of various bitumen. It can be found that linear chemo-mechanics of bitumen exist and are independent on the bitumen type

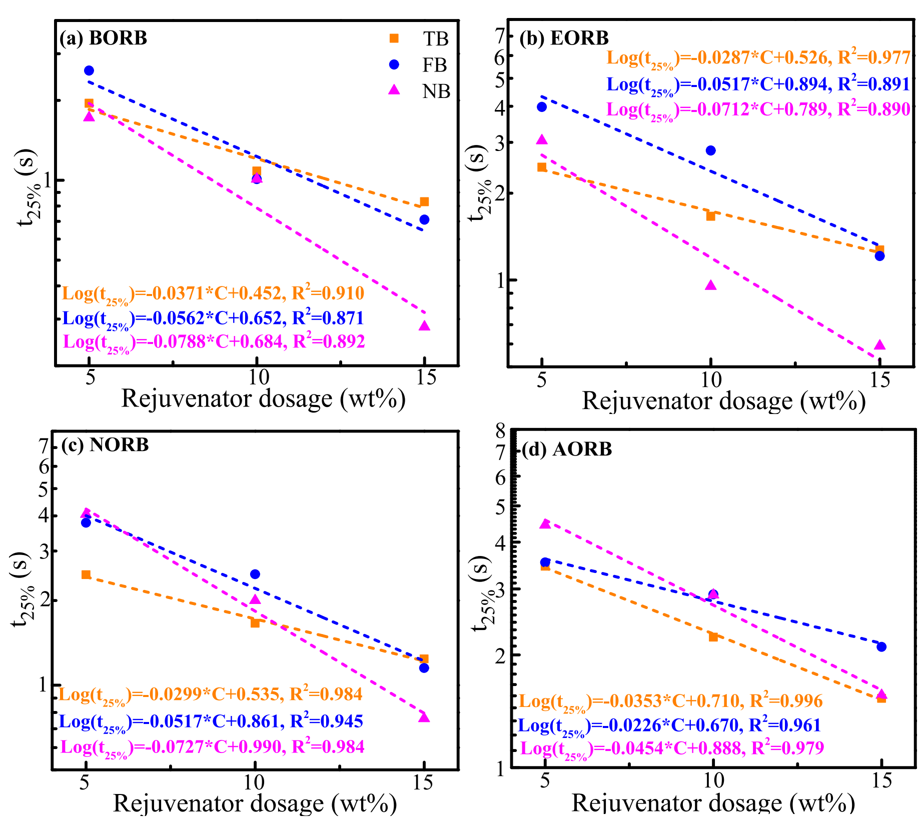

Fig. 12. Effect of bitumen type on the $t_{25\%}$ values of rejuvenated bitumen.

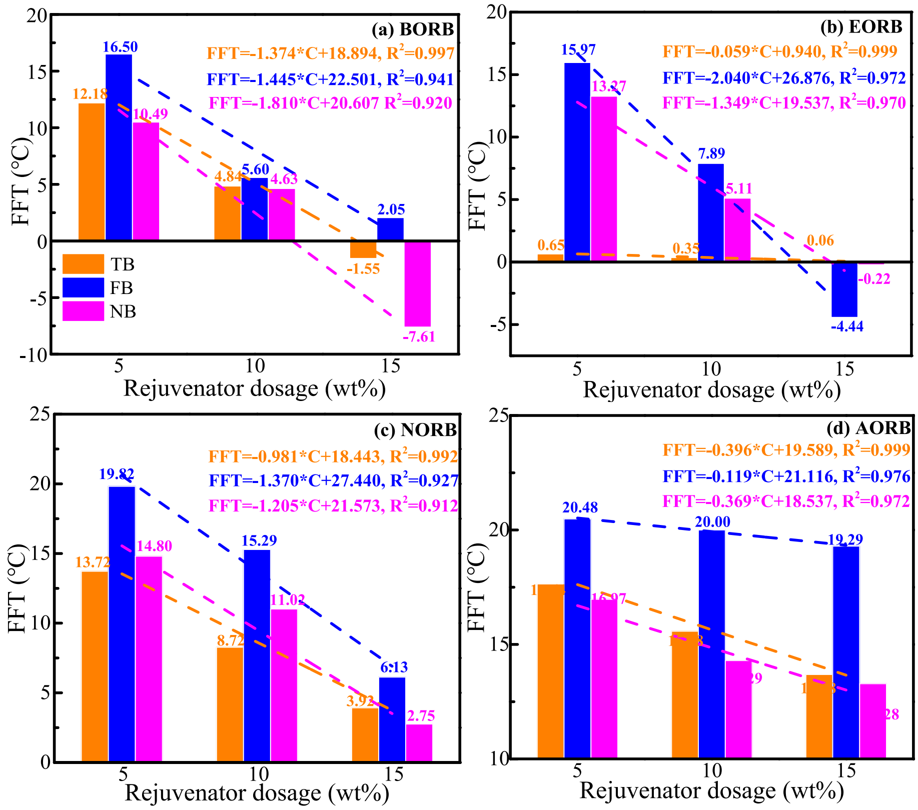

Fig. 13. Effect of bitumen type on the FFT values of rejuvenated bitumen.

and aging level. The bitumen with low CI and high A% shows a lower FFT value and better fatigue resistance. Meanwhile, the increase in oxygen content significantly reduces the fatigue life of bitumen, while the H% shows a slight improvement effect, verifying the N_f result shown in Fig. 5(b). Nevertheless, the significant fluctuations in correlation curves are observed because the rheological index of bitumen is the result of joint actions between various chemical properties. Thus, it is necessary to explore the pluralistic chemo-mechanics of bitumen using machine learning tool, which will be presented in section 3.3.

3.2. Effects of rejuvenator type and bitumen source on rejuvenated bitumen

3.2.1. High-temperature properties

The combined effects of bitumen type, rejuvenator type and dosage on the high-temperature properties (RFT and $J_{nr3.2}$) are shown in Fig. 9 and Fig. 10, respectively. For all bitumen and rejuvenator sources, the RFT index of rejuvenated bitumen declines linearly and the Log($J_{nr3.2}$) value increases linearly as the increment in rejuvenator dosage. It indicates that the deteriorating impact of rejuvenator on the high-temperature performance of aged bitumen is independent on the bitumen and rejuvenator types. Regardless of rejuvenator type and dosage, the NB rejuvenated bitumen present the lowest RFT values because of its smallest asphaltene dosage, while the TB and FB rejuvenated bitumen show the similar high-temperature deformation resistance. As the increase of bio-oil content, the decreasing rate in RFT value of FB rejuvenated bitumen is stronger than the TB and NB ones. For other three rejuvenators (EO, NO, and AO), the NB bitumen exhibits the fastest reduction rate in RFT values, followed by the FB and TB. This is related to low asphaltene content in NB bitumen, and incorporating rejuvenator further increases the intermolecular distance and weakens the intermolecular forces between asphaltene molecules.

As shown in Fig. 10, all FB rejuvenated bitumen display the lowest $J_{nr3.2}$ values, while the NB bitumen have a slightly higher $J_{nr3.2}$ than the TB ones. It means that the FB bitumen presents the best high-temperature deformation resistance, while NB bitumen show the worst behavior. The ranking in increasing effect of rejuvenators on $J_{nr3.2}$ values is Bio-oil > Engine-oil > Naphthenic-oil > Aromatic-oil, regardless of rejuvenator dosage and bitumen source. Thus, the softening ranking of different rejuvenators on aged bitumen is independent on the bitumen sources. However, the impact of rejuvenator dosage on $J_{nr3.2}$ value of rejuvenated bitumen is affected by both rejuvenator type and bitumen source. For the rejuvenators BO, EO, and NO, the increasing rate of $J_{nr3.2}$ parameters versus rejuvenator dosage for FB and NB bitumen are faster than the TB bitumen, while a converse finding is observed for the AO rejuvenator. Therefore, it is challenging to draw a general conclusion on rejuvenation efficiency of rejuvenated bitumen due to the combined effects of different influence factors (bitumen components, rejuvenator type/dosage, and their interactions). The rejuvenation primarily softens the aged bitumen by increasing molecular spacing and weakening van der Waals interactions between asphaltene particles. The extent of this disruption depends not only rejuvenator polarity and molecular size but also on the original asphaltene content and structure of aged bitumen [16,38].

3.2.2. Relaxation properties

The relaxation results (τ_{50s} and $t_{25\%}$) of all rejuvenated bitumen are plotted in Fig. 11 and Fig. 12, respectively. The increase in rejuvenator dosage results in a linear reduction of τ_{50s} and $t_{25\%}$ values, which are converse to the aging effect. It means that all rejuvenators show great effects on restoring the low-temperature relaxation performance of aged bitumen. It is noticed that the FB rejuvenated bitumen always have the higher τ_{50s} values than the TB and NB bitumen, showing that the FB bitumen presents a worse relaxation capacity. It agrees well with the high-temperature performance result, which is due to the more significant elastic performance of FB bitumen. However, the decreasing rate of τ_{50s} index as a function of rejuvenator content is affected by both rejuvenator type and bitumen source. For all bitumen types, the ranking in

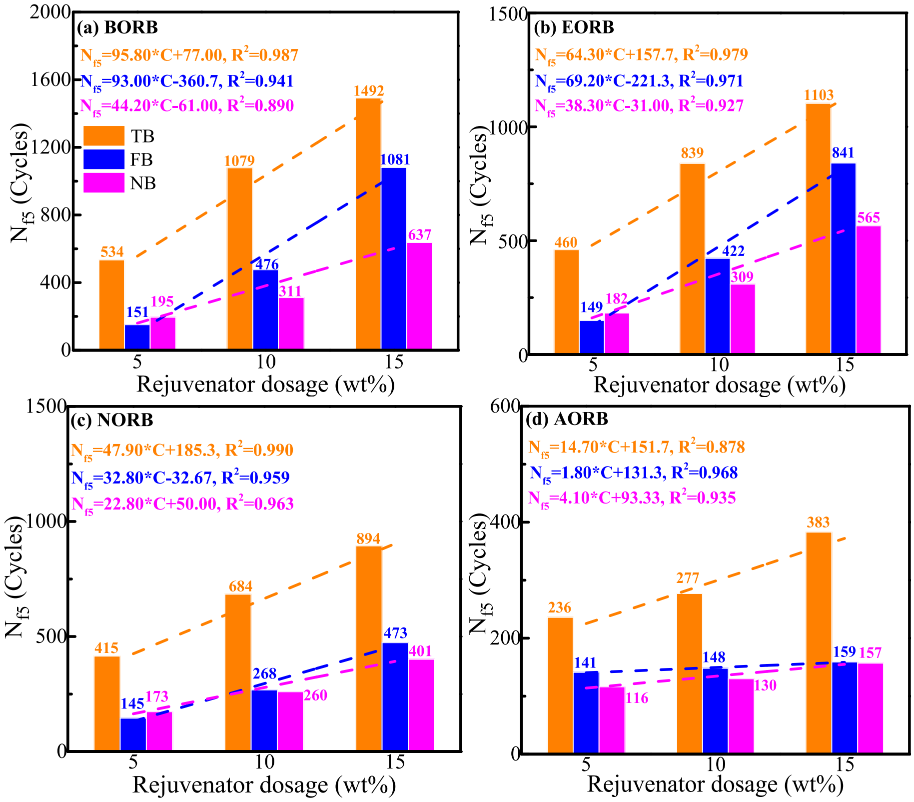

Fig. 14. Effect of bitumen type on the N_{f5} values of rejuvenated bitumen.

sensitivity level of τ_{50s} values to rejuvenator dosage is BORB < EORB < NORB, but the AORB depends on the bitumen source.

From Fig. 12, it can be seen that the relaxation time of rejuvenated bitumen is affected by all influence factors (rejuvenator type and dosage, and bitumen source). For all rejuvenated bitumen, their $t_{25\%}$ values show linear reduction trend as the increase of rejuvenator dosage, and the decreasing rate of NB bitumen is the largest. Thus, the $t_{25\%}$ of NB bitumen has the most sensitive to the rejuvenator dosage for all four rejuvenators. For rejuvenators BO, EO, and NO, the $t_{25\%}$ values of TB rejuvenated bitumen presents a lower decreasing rate than the FB bitumen, but an opposite phenomenon is observed for rejuvenator AO. It is necessary to adopt advanced data analysis method to accurately predict the relaxation performance of rejuvenated bitumen, considering all influence factors of bitumen source, aging level of bitumen, rejuvenator type and dosage. From the mechanistic standpoint, the observed improvement in relaxation performance is attributed to the enhanced mobility of polymeric chains and the suppression of glassy segment behaviour in aged bitumen. Rejuvenators with lower viscosity and higher maltene compatibility (e.g., bio-oil) diffuse more effectively into aged bitumen, plasticizing the matrix and facilitating stress relaxation under thermal and mechanical loading [16,39].

3.2.3. *Fatigue properties*

The fatigue failure temperature (FFT) results of all rejuvenated bitumen are illustrated in Fig. 13. As the increase in rejuvenator dosage, all FFT values tend to decrease linearly. It means that adding rejuvenator improves the fatigue resistance of aged bitumen. The enhancement in fatigue life is a result of rejuvenator-facilitated molecular rearrangement, which reduces brittleness and restores energy dissipation capacity under cyclic loading [16,51].

However, this improvement effect is dependent on both bitumen source and rejuvenator type. Apart from the EORB with FB bitumen and EO dosage of 15 %, the FFT values of all FB-based rejuvenated bitumen are larger than the TB ad NB-based bitumen. It implies that the FB bitumen show the lowest fatigue resistance. Additionally, the FFT values of TB-based rejuvenated bitumen with rejuvenators bio-oil and aromatic-oil are higher than NB-based ones. However, one opposite trend is observed for other two cases (rejuvenators engine-oil and naphthenic-oil). After comparing the FFT values, it is revealed that the bio-oil is more efficient for enhancing the fatigue performance of NB-based aged bitumen, while engine-oil is more suitable for both TB and FB-based aged bitumen.

The fatigue life N_{f5} values of all rejuvenated bitumen are displayed in Fig. 14. Regardless of bitumen and rejuvenator type, the fatigue life of rejuvenated bitumen increases linearly as a function of rejuvenator dosage. However, this improvement effect is dependent on both rejuvenator type and bitumen source. The bio-oil rejuvenated bitumen exhibits highest fatigue life for all three bitumen sources, which differs from the finding based on FFT parameter. Thus, the fatigue performance evaluation of rejuvenated bitumen also depends on the parameter type. The best evaluation parameter should be further determined by connecting these bitumen-level rankings with mixture-level results. Moreover, the TB-based rejuvenated bitumen exhibits the largest N_{f5} values, indicating the TB bitumen shows the longer fatigue life than the FB and NB bitumen. It seems to contradict the FFT results showing the fatigue resistance ranking as NB > TB > FB, which can be attributed to the fundamental differences between the two fatigue tests. The FFT result is from the linear viscoelastic domain and primarily captures early-stage stiffness-related behaviour and may not reflect damage evolution mechanisms of bitumen. As a result, its sensitivity to compositional differences in cracking behaviour among binders is limited. In contrast, the LAS test assesses binder response under progressive strain amplitudes, enabling the evaluation of crack initiation and growth. This makes LAS test more capable of capturing the cumulative fatigue behaviour of bitumen with varying chemical and rheological properties, thereby providing a more reliable comparison of fatigue resistance across different bitumen types. For rejuvenators bio-oil and engine-oil, the FB-based rejuvenated bitumen presents much higher fatigue life

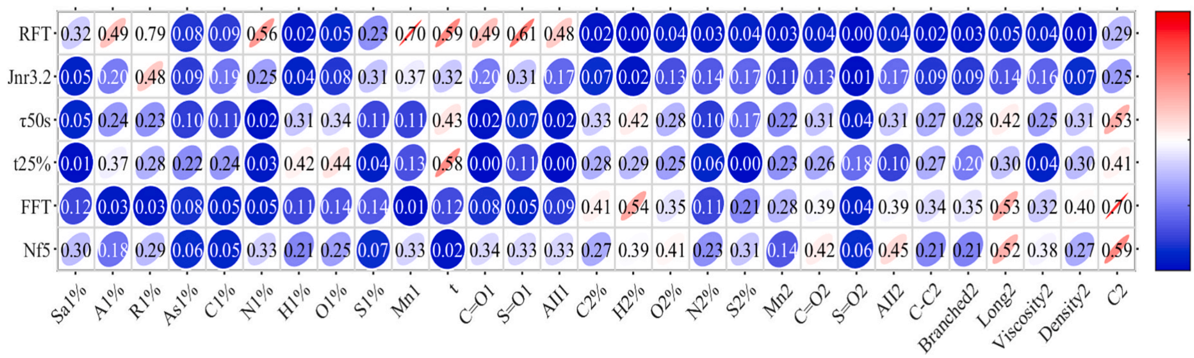

Fig. 15. Absolute correlation distribution between rheological and chemical indices.

Table 4
The most relevant chemical indices to various rheological properties.

High-temperature performance	RFT (°C)	R1 (%)	N1 (%)	M_n1 ($g{\cdot}mol^{-1}$)	t (h)	S=O1
	$J_{nr3.2}$ (kPa^{-1})	R1 (%)	S1 (%)	M_n1 ($g{\cdot}mol^{-1}$)	t (h)	S=O1
Low-temperature performance	τ_{50s} (Pa)	O1 (%)	t (h)	H2 (%)	Long 2	C2
	$t_{25\%}$ (Pa)	A1 (%)	H1 (%)	O1 (%)	t (h)	C2
Fatigue performance	FFT (°C)	C2 (%)	H2 (%)	Long2	ρ2 ($g{\cdot}cm^{-3}$)	C2
	N_f (cycles)	O2 (%)	C=O2	AII2	Long2	C2

than the NB-based bitumen, but the difference is not significant for naphthenic-oil and aromatic-oil rejuvenators. Based on the LAS fatigue results, the bio-oil is the best rejuvenator for prolonging the fatigue life of aged bitumen, especially for TB and FB-based bitumen.

3.3. Machine learning analysis on chemo-rheological connections

3.3.1. Initial analysis on chemo-rheological correlation

To initially analyze the potential connection between all chemical and rheological indices of fresh, aged, and rejuvenated bitumen, the Pearson correlation method was adopted and the correlation result is displayed in Fig. 15. It should be mentioned that "1″ represents the chemical characteristics of aged bitumen, while "2" refers to the rejuvenator property. Meanwhile, other two input parameters, aging time (t) and rejuvenator dosage (C2), were also considered. Based on the Pearson correlation results, five most relevant chemical indices for different rheological parameters of all fresh, aged, and rejuvenated bitumen are selected and summarized in Table 4.

It is observed that the RFT index of rejuvenated bitumen is closely related to resin fraction (R1), nitrogen dosage (N1), molecular weight (Mn1), aging time (t) and sulfoxide index (S=O1) of aged bitumen with the correlation coefficient R^2 value of 0.79, 0.56, 0.70, 0.59, and 0.61, respectively. The $J_{nr3.2}$ index also shows high correlation levels with these input parameters, except for the N1 (replaced by S1). However, the correlation degree for $J_{nr3.2}$ is lower than RFT. Regarding the low-temperature performance, there are potential connections between the τ_{50s} and oxygen dosage (O1) and t of aged bitumen, as well as the hydrogen content (H2), Long-chain index (Long2), and dosage (C2) of rejuvenator. Apart from O1, t, and C2, the $t_{25\%}$ has a certain relevancy with aromatic fraction (A1) and hydrogen dosage (H1) of aged bitumen. Furthermore, both fatigue indices (FFT and N_f) are closer linked to rejuvenator properties than the aged bitumen. In detailed, the C2 and Long2 indices affect the FFT and N_f results of rejuvenated bitumen. The FFT parameter links well to carbon dosage (C2), hydrogen dosage (H2), and density (ρ2) of rejuvenator, while the N_f index shows potential correlations with oxygen dosage (O2), carbonyl index (C=O2), and aromaticity index (AII2) of rejuvenator.

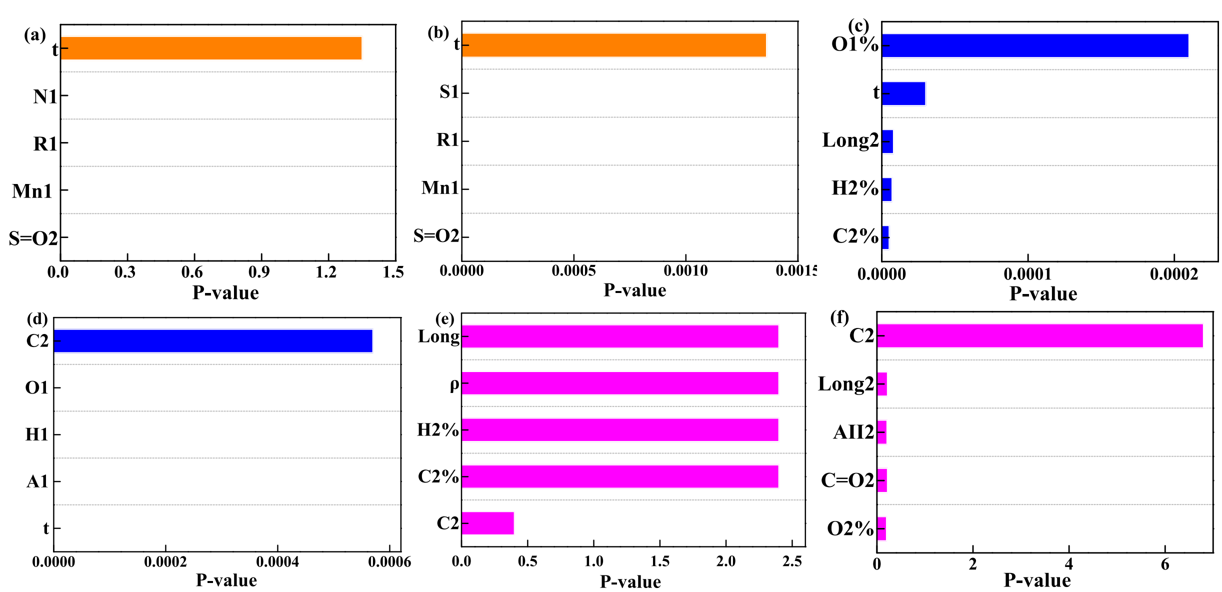

Fig. 16. P-values of different chemical indices from ANOVA method: (a) RFT, (b) $J_{nr3.2}$, (c) τ_{50s}, (d) $t_{25\%}$, (e) FFT, and (f) N_{f5}.

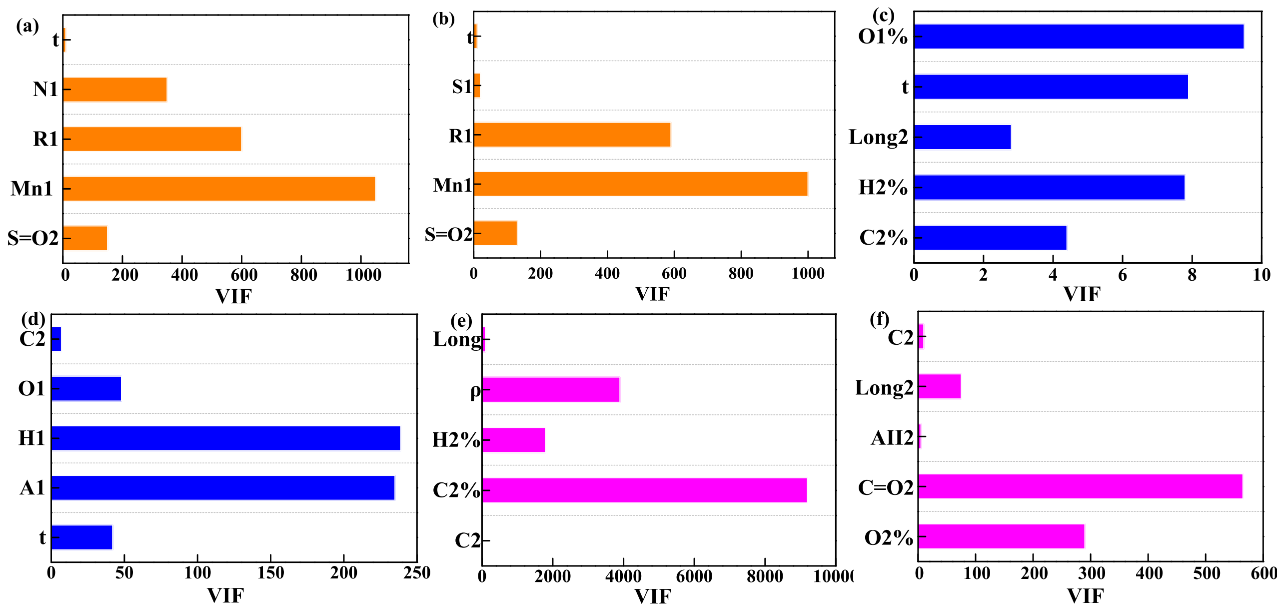

Fig. 17. VIF values of various chemical indices from ANOVA method: (a) RFT, (b) $J_{nr3.2}$, (c) τ_{50s}, (d) $t_{25\%}$, (e) FFT, and (f) N_{f5}.

3.3.2. Analysis of variance (ANOVA)

To assess the significance of different chemical factors on the rheological properties of rejuvenated bitumen with variable bitumen and rejuvenator sources, aging level of bitumen, and rejuvenator dosage, the ANOVA method was first adopted and two parameters (P-value and VIF) are derived. Their results are illustrated in Fig. 16 and Fig. 17, respectively. It should be mentioned that the input parameter with a lower P-value will show more important to the output index. It is observed that compared to other relevant chemical indicators, the aging time (t) shows less important to affect the high-temperature properties (RFT and $J_{nr3.2}$) of all fresh, aged, and rejuvenated bitumen. However, the t index for $J_{nr3.2}$ is more significant than RFT.

Regarding the low-temperature indices (τ_{50s} and $t_{25\%}$), the P-values for all input parameters are lower than 0.0002. It means that these chemical parameters are closely correlated to the relaxation performance of rejuvenated bitumen. The order for influence level of these parameters to τ_{50S} is C2% > H2% > Long2 > t > O1%, while C2 shows lower influence effect on $t_{25\%}$ result than other input parameters (O1, H1, A1, and t). The P values between the FFT and four chemical indices (Long2, ρ2, H2, and C2%) are higher than that of C2, indicating that the rejuvenator dosage has the largest effect on FFT. However, the rejuvenator dosage shows the lower influence level on N_f index than Long2, AII2, C=O2, and O2%.

The variance inflation factor (VIF) values are plotted in Fig. 17. A higher VIF value indicates a greater degree of multicollinearity, implying that the corresponding independent variables are strongly correlated with one another [52]. For RFT and $J_{nr3.2}$, the VIF values of R1, Mn1, and S=O2 exceed 100, suggesting significant multicollinearity among these chemical indicators. In contrast, the aging time (t) appears to be independent of the other variables. The VIF values of Long2 and C2% to τ_{50s} are lower than 5.0, showing their independent characteristic. However, multicollinearity is evident among the O1%, t, and H2% indices. According to the large VIF values, it is concluded that all input parameters for $t_{25\%}$ are dependent each other. Additionally, the C2 index

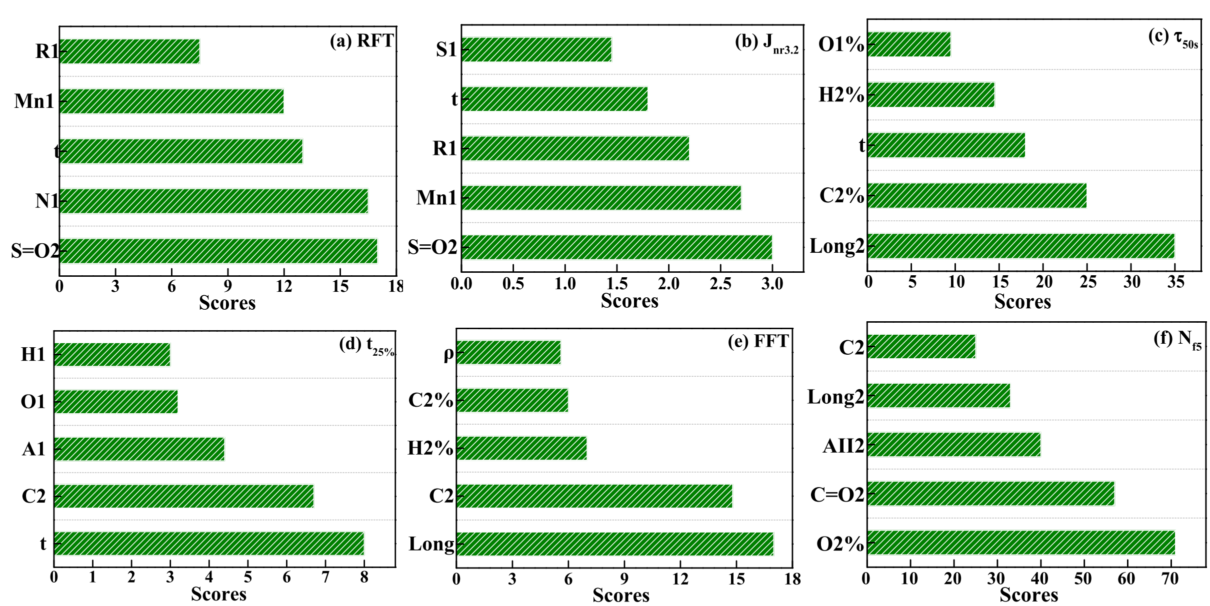

Fig. 18. Importance scores of various chemical indices from Chi-square test.

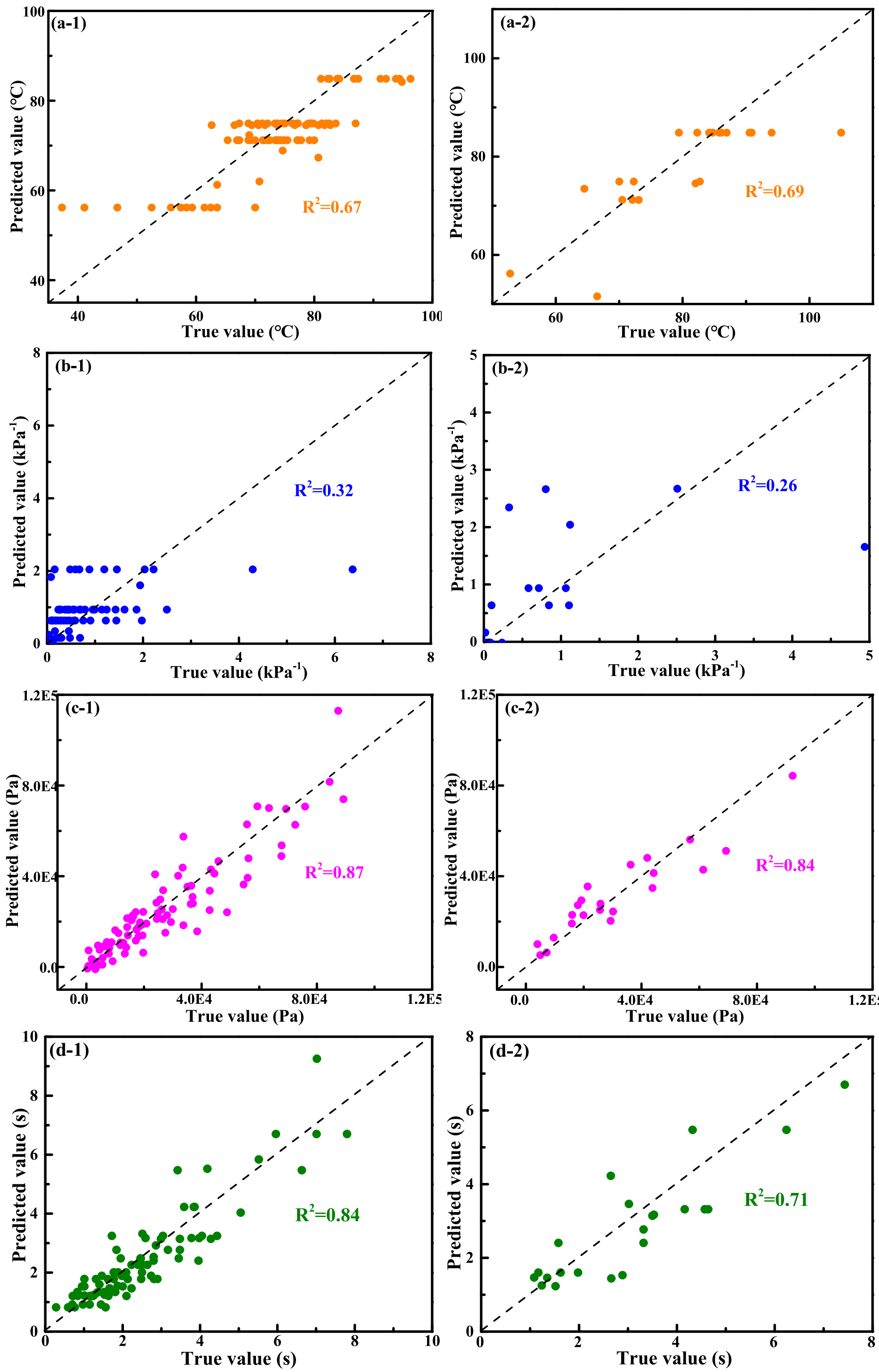

Fig. 19. The fitting efficiency of ANN method on different rheological indicators (a-1)(a-2) RFT, (b-1)(b-2) $J_{nr3.2}$, (c-1)(c-2) τ_{50s}, (d-1)(d-2) $t_{50\%}$, (e-1)(e-2) FFT, (f-1)(f-2) N_{f5}.

is independent in both FFT and N_{f5} models, while Long2 and AII2 also act as independent variables in their respective cases.

3.3.3. Chi square test

The Chi-square test was adopted to evaluate and distinguish the importance scores of different chemical indices to high-temperature deformation, low-temperature relaxation, and fatigue performance of fresh, aged, and rejuvenated bitumen. The importance score distributions are presented in Fig. 18. Obviously, one chemical parameter with a higher score will show more significant effect on rheological index [53].

The relative importance of chemical parameters to RFT follows the order: S=O2 > N1 > t > Mn1 > R1, and these parameters exhibit a lower

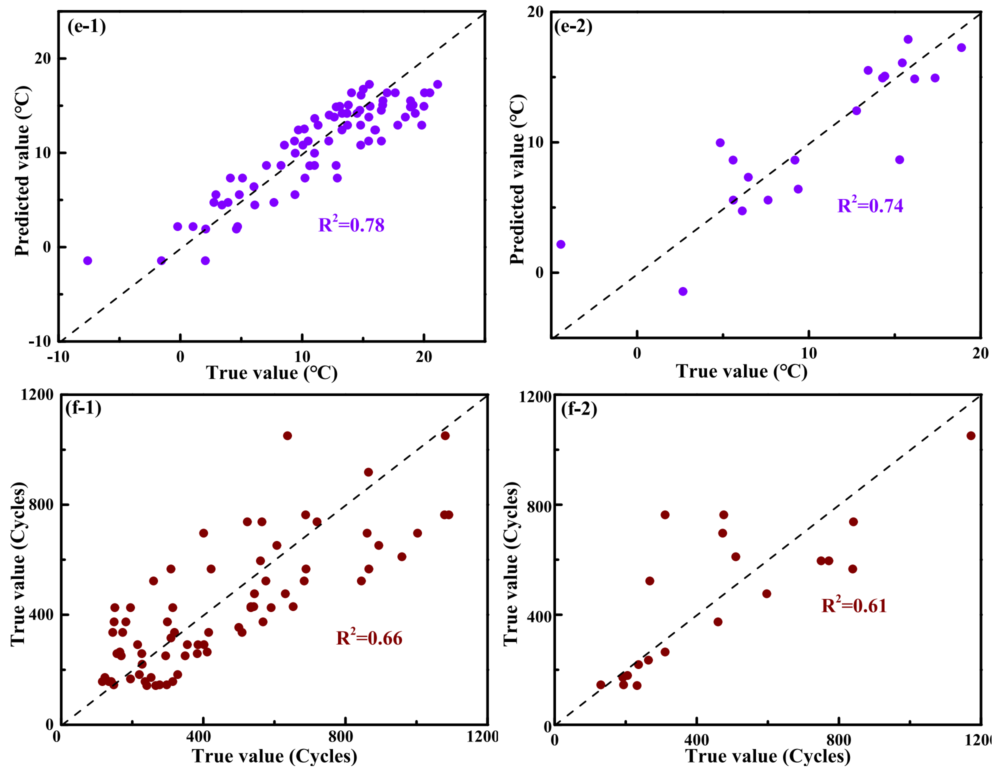

Fig. 19. (*continued*).

influence degree on $J_{nr3.2}$ index. The relaxation parameter τ_{50s} is most strongly affected by the Long-aliphatic index, followed by carbon dosage of rejuvenator (C2%), aging time (t), hydrogen dosage of rejuvenator (H2%), and oxygen dosage of bitumen (O1%). For the relaxation time $t_{25\%}$, aging time (t) emerges as the most influential factor among all chemical indicators. Regarding the FFT parameter, the Long-aliphatic index shows the largest importance level, followed by rejuvenator dosage (C2), carbon, hydrogen contents and density of rejuvenator. For N_{f5} index, the ranking of importance score for various chemical inputs is C2 < Long2 < AII2 < C=O2 < O2%.

3.3.4. Artificial neural network (ANN) modelling

The rheological properties of fresh, aged, and rejuvenated bitumen are modelled using an Artificial neural network (ANN), with the input parameters summarized in Table 4. The prediction results are presented in Fig. 19. For each rheological index, the left-side plot shows the ANN performance on the training dataset, while the right-side plot reflects the validation dataset results. In this study, the ANN model shows limited predictive capacity for high-temperature performance indices, and the training efficiency R^2 values for RFT and $J_{nr3.2}$ are only 0.69 and 0.26, respectively. Thus, the developed ANN model is not suitable for accurately predicting high-temperature behaviour of bitumen, particularly for the $J_{nr3.2}$ index.

However, Fig. 19(c) and (d) demonstrate that the predicted values for both relaxation stress (τ_{50s}) and relaxation time ($t_{50\%}$) show good agreement with the experimental results, achieving high R^2 value of 0.84 and 0.71, respectively. It indicates that the proposed ANN model is effective in predicting the low-temperature relaxation performance of fresh, aged, and rejuvenated bitumen based on their chemical characteristics, regardless of bitumen aging level, rejuvenator type and dosage. Compared to $t_{50\%}$, the prediction efficiency for τ_{50s} is more significant.

The prediction results for the fatigue properties, fatigue failure temperature (FFT) and fatigue life (N_f), are shown in Fig. 19(e) and (f). The predicted values align reasonably well with the experimental data, yielding R^2 values of 0.74 and 0.61, respectively. Thus, the proposed ANN model is capable of predicting fatigue-related parameters of fresh, aged, and rejuvenated bitumen based on chemical input variables. Although the prediction efficiency of this ANN model on fatigue performance is better on high-temperature indicators, it is worse than the low-temperature relaxation indices. Overall, the developed ANN model shows the highest applicability for relaxation indices, followed by fatigue and rutting properties.

4. Conclusions and recommendations

This study systematically investigates the effects of bitumen source, rejuvenator type and dosage on the chemical and rheological performance of rejuvenated bitumen. Statistical analyses and machine learning techniques are used to explore chemo-mechanical relationships, leading to the following key findings:

(1) SARA analysis shows that NB bitumen retains the lowest asphaltene content (10.9 %) after 80-hours aging, indicating superior aging resistance compared to TB (25.4 %) and FB (31.6 %). FB bitumen contains the highest sulfur content, resulting in a more pronounced oxygen increase upon aging. The molecular weight evolution (M_w and M_n) also varies by bitumen type, with TB showing the highest susceptibility to aging.

(2) TB bitumen exhibits the best rutting resistance but poor relaxation, while fatigue resistance ranks as TB > FB > NB. Strong correlations are observed between key rheological parameters and chemical indices, such as RFT with colloidal instability index (CI, $R^2 = 0.88$) and asphaltene content ($R^2 = 0.86$), and relaxation indices (τ_{50s} and $t_{25\%}$) with aromatic content (A%) and CI. The FFT index is also closely linked to A% (0.84) and CI, while other fatigue parameters (N_f, ε_{sr}, and E) correlate well with O% and H%.

(3) NB-rejuvenated bitumen has the lowest RFT values due to limited asphaltene content, while TB and FB-rejuvenated bitumen show similar high-temperature deformation resistance. However, FB-

rejuvenated bitumen shows the weakest relaxation capacity, influenced by rejuvenator type and bitumen source. Relaxation stress sensitivity to rejuvenator dosage ranks as BORB < EORB < NORB across bitumen types, with AORB varying by source. LAS fatigue tests confirm that bio-oil is most effective in improving fatigue life, especially for TB and FB bitumen.

(4) The developed ANN model is effective in accurately predicting the rheological properties of rejuvenated bitumen based on various chemical input parameters. Its highest applicability is seen in predicting relaxation indices, followed by its effectiveness in forecasting fatigue and rutting properties.

(5) The findings offer a scientific basis for selecting rejuvenators based on the specific aging level and bitumen type. Bio-oil is recommended for highly aged binders with poor fatigue resistance, such as TB and FB bitumen. Aromatic oils may require source-specific validation, and rejuvenator dosage should also be carefully optimized to balance high-temperature and low-temperature performance.

In future work, these key evaluation indicators for rejuvenated bitumen proposed from this study should be further optimized through rejuvenation efficiency evaluation on recycled asphalt mixtures. Moreover, more database from other bitumen sources and rejuvenator types will be collected and involved to improve the artificial neural network (ANN) modelling for more accurate prediction.

CRediT authorship contribution statement

Shisong Ren: Writing – original draft, Methodology, Investigation, Formal analysis, Data curation. **Mahmoud Khadijeh:** Writing – review & editing, Methodology, Data curation. **Eli I. Assaf:** Writing – review & editing, Investigation, Data curation. **Xueyan Liu:** Writing – review & editing, Supervision, Methodology. **Sandra Erkens:** Writing – review & editing, Supervision, Funding acquisition.

Declaration of competing interest

The authors declare that they have no known competing financial interests or personal relationships that could have appeared to influence the work reported in this paper.

Acknowledgement

The authors would thank the funding support from the research program Knowledge-based Pavement Engineering (KPE), and the first author would appreciate the funding support from the Research Foundation-Flanders (FWO, Belgium) with postdoc fellowship [1202125 N].

Data availability

Data will be made available on request.

References

[1] M. Khorshidi, M. Ameri, A. Goli, Cracking performance evaluation and modelling of RAP mixtures containing different recycled materials using deep neural network model, Road Mater. Pavement Des. (2023).
[2] T. Tian, Y. Jiang, S. Li, C. Nie, Y. Yi, Y. Zhang, C. Deng, Bending fatigue properties and prediction of asphalt mixtures with ultra-large aggregates, Constr. Build. Mater. 414 (2024) 134961.
[3] K. Schwettmann, N. Nytus, S. Weigel, M. Radenberg, D. Stephan, Effects of rejuvenators on bitumen ageing during simulated cyclic reuse: a review, Resour. Conserv. Recycl. 190 (2023) 106776.
[4] J. Liu, Z. Wang, R. Luo, G. Bian, Q. Liang, F. Yan, Changes of components and rheological properties of bitumen under dynamic thermal aging, Constr. Build. Mater. 3030 (2021) 124501.
[5] Z. Li, C. Fa, H. Zhao, Y. Zhang, H. Chen, H. Xie, Investigation on evolution of bitumen composition and micro-structure during aging, Constr. Build. Mater. 244 (2020) 118322.
[6] M. Aliha, S. Shaker, Effect of bitumen type, temperature and aging on mixed I/II fracture toughness of asphalt binders-experimental and theoretical assessment, Theor. Appl. Fract. Mech. 110 (2020) 102801.
[7] E. Goosen, K. Jenkins, Understanding bitumen aging through interrelationships and aging ratios, Transp. Res. Rec. 1–26 (2023).
[8] Z. Chen, H. Zhang, X. Liu, H. Duan, A novel method for determining the time-temperature superposition relationship of SBS modified bitumen: Effects of bitumen source, modifier type and aging, Constr. Build. Mater. 280 (2021) 122549.
[9] B. Gomez-Meijide, H. Ajam, A. Garcia, S. Vansteenkiste, Effect of bitumen properties in the induction healing capacity of asphalt mixes, Constr. Build. Mater. 190 (2018) 131–139.
[10] P. Redelius, H. Soenen, Relation between bitumen chemistry and performance, Fuel 140 (2015).
[11] A. Khiavi, S. Naseri, The effect of bitumen types on the performance of high-modulus asphalt mixtures, Pet. Sci. Technol. 37 (2019) 1223–1230.
[12] Z. Han, P. Cong, J. Qiu, Microscopic experimental and numerical research on rejuvenators: a review, Journal of Traffic and Transportation Engineering (english Edition). 9 (2) (2022) 180–207.
[13] A. Behnood, Application of rejuvenators to improve the rheological and mechanical properties of asphalt binders and mixtures: a review, J. Clean. Prod. 231 (2019) 171–182.
[14] J. Yi, Y. Wang, Z. Pei, M. Xu, D. Feng, Mechanisms and research progress on biological rejuvenators for regenerating aged asphalt: Review and discussion, J. Clean. Prod. 422 (2023) 138622.
[15] S. Ren, X. Liu, A. Varveri, S. Khalighi, R. Jing, S. Erkens, Aging and rejuvenation effects on the rheological response and chemical parameters of bitumen, J. Mater. Res. Technol. 25 (2023) 1289–1313.
[16] S. Ren, X. Liu, S. Erkens, Role of thermodynamic relaxation on effectiveness of recycling agents on properties of aged bitumen, Fuel 368 (2024) 131658.
[17] R. Ahmed, K. Hossain, M. Aurilio, R. Hajj, Effect of rejuvenator type and dosage on rheological properties of short-term aged binders, Mater. Struct. 54 (2021) 109.
[18] A. Gamarra, E. Ossa, Thermo-oxidative aging of bitumen, Int. J. Pavement Eng. 19 (7) (2018) 641–650.
[19] G. Pipintakos, H. Soenen, H. Ching, C. Velde, S. Doorslaer, F. Lemiere, A. Varveri, W. Van den bergh, Exploring the oxidative mechanisms of bitumen after laboratory short- and long-term ageing, Constr. Build. Mater. 289 (2021) 123182.
[20] E. Fini, S. Hosseinnezhed, D. Oldham, E. Chailleux, V. Gaudefroy, Source dependency of rheological and surface characteristics of bio-modified asphalts, Road Mater. Pavement Des. 18 (2) (2017) 408–424.
[21] J. Zhu, B. Birgisson, N. Kringos, Polymer modification of bitumen: advances and challenges, Eur. Polym. J. 54 (2014) 18–38.
[22] G. Pipintakos, A. Sreeram, J. Mirwald, A. Bhasin, Engineering bitumen for future asphalt pavements: a review of chemistry, structure and rheology, Mater. Des. 244 (2024) 113157.
[23] X. Ma, X. Ma, Z. Wang, S. Song, Y. Sheng, Investigation of changing SARA and fatigue properties of asphalt bitumen under ageing and analysis of their relation based upon the BP neural network, Constr. Build. Mater. 394 (2023) 132163.
[24] R. Botella, D. Presti, K. Vasconcelos, K. Bernatowicz, A. Martinez, R. Miro, L. Specht, E. Mercado, G. Pires, E. Pasquini, C. Ogbo, F. Preti, M. Pasetto, A. Carrion, A. Roberto, M. Oreskovic, K. Kuna, G. Guduru, A. Martin, A. Carter, G. Giancontieri, A. Abed, E. Dave, G. Tebaldi, Machine learning techniques to estimate the degree of binder activity of reclaimed asphalt pavement, Mater. Struct. 55 (2022) 112.
[25] S. Salehi, M. Arashpour, E. Golafshani, J. Kodikara, Prediction of rheological properties and ageing performance of recycled plastic modified bitumen using machine learning models, Constr. Build. Mater. 401 (2023) 132728.
[26] L. Shan, Y. Wang, S. Liu, X. Qi, J. Wang, Establishment of correlation model between compositions and dynamic viscoelastic properties of asphalt binder based on machine learning, Constr. Build. Mater. 364 (2023) 129902.
[27] B. Asadi, R. Hajj, Prediction of asphalt binder elastic recovery using tree-based ensemble bagging and boosting models, Constr. Build. Mater. 410 (2024) 134154.
[28] ASTM D5. Standard Test Method for Penetration of Bituminous Materials.
[29] ASTM D36. Standard Test Method for Softening Point of Bitumen (Ring and Ball apparatus).
[30] AASHTI M320. Standard Specification for Performance-graded Asphalt Binder.
[31] EN 15326. British Standard for Bitumen and Bituminous Binders-Measurement of Density and Specific Gravity-Capillary-Stoppered Pycnometer Method.
[32] AASHTO T316. Standard Method of Test for Viscosity Determination of Asphalt Binder Using Rotational Viscometer.
[33] ASTM D93. Standard Test Methods for Flash Point by Pensky-Martens Closed Cup Tester.
[34] ASTM D7343. Standard Practice for Optimization, Sample Handling, Calibration, and Validation of X-ray Fluorescence Spectrometry Methods for Elemental Analysis of Petroleum Products and Lubricants.
[35] ASTM UOP676. Molecular Weight by Vapor Pressure Osmometry.
[36] S. Ren, X. Liu, M. Aggelen, P. Lin, S. Erkens, Do different chemical and rheological properties act as effective and critical indicators for efficiency evaluation of rejuvenated bitumen? Constr. Build. Mater. 411 (2024) 134774.
[37] S. Ren, X. Liu, P. Lin, S. Erkens, Y. Xiao, Chemo-physical characterization and molecular dynamics simulation of long-term aging behaviors of bitumen, Constr. Build. Mater. 302 (2021) 124437.
[38] S. Ren, X. Liu, S. Erkens, Unraveling the critical indictors for evaluating the high-temperature performance of rejuvenator-aged bitumen blends, Case Stud. Constr. Mater. 19 (2023) e02522.

[39] S. Ren, X. Liu, S. Erkens, Towards critical low-temperature relaxation indicators for effective rejuvenation efficiency evaluation of rejuvenator-aged bitumen blends, J. Clean. Prod. 426 (2023) 139092.

[40] G. Li, C. Qi, S. Han, L. Fan, D. Kuang, H. Chen, Y. Wu, Effects of cutting temperature on the genes and fatigue properties of asphalt during its refining process, Fuel 375 (2024) 132602.

[41] Z. Liu, L. Sun, J. Li, L. Liu, Effect of key design parameters on high temperature performance of asphalt mixtures, Constr. Build. Mater. 348 (2022) 128651.

[42] C. Varanda, I. Portugal, J. Ribeiro, A. Silva, C. Silva, Optimization of bitumen formulations using mixture design of experiments (MDOE), Constr. Build. Mater. 156 (2017) 611–620.

[43] S. Aflaki, M. Memarzadeh, Using two-way ANOVA and hypothesis test in evaluating crumb rubber modification (CRM) agitation effects on rheological properties of bitumen, Constr. Build. Mater. 25 (4) (2011) 2094–2106.

[44] A. Sharma, G. Ransinchung, P. Kumar, Applicability of various mixing rules for hot asphalt recycled binders, Road Mater. Pavement Des. 23 (11) (2022) 2547–2566.

[45] F. Pedregosa, G. Varoquaux, A. Gramfort, V. Michel, B. Thirion, O. Grisel, M. Blondel, P. Prettenhofer, R. Weiss, V. Dubourg, J. Vanderplas, A. Passos, D. Cournapeau, M. Brucher, M. Perrot, E. Duchesnay, Scikit-learn: Machine Learning in Python, Journal of Machine Leaning Research. 12 (2011) 2825–2830.

[46] Nair. V., Hinton. G. Rectified linear units improve restricted Boltzmann machines. Proceedings of the 27th International Conference on Machine Learning (ICML-10). 2010, 807-814.

[47] L. Ma, A. Varveri, R. Jing, S. Erkens, Chemical characterisation of bitumen type and ageing state based on FTIR spectroscopy and discriminant analysis integrated with variable selection methods, Road Mater. Pavement Des. 24 (S1) (2023) S506–S520.

[48] K. Primerano, J. Mirwald, B. Hofko, Asphaltenes and maltenes in crude oil and bitumen: a comprehensive review of properties, separation methods, and insights into structure, reactivity and aging, Fuel 368 (2024) 131616.

[49] D. Lesueur, The colloidal structure of bitumen: Consequences on the rheology and on the mechanisms of bitumen modification, Adv. Colloid Interface Sci. 145 (2009) 42–82.

[50] X. Lu, H. Soenen, P. Sjovall, G. Pipintakos, Analysis of asphaltenes and maltenes before and after long-term aging of bitumen, Fuel 304 (2021) 121426.

[51] S. Ren, X. Liu, S. Erkens, Insight into the critical evaluation indicators for fatigue performance recovery of rejuvenated bitumen under different rejuvenation conditions, Int. J. Fatigue 175 (2023) 107753.

[52] N. Panchev, K. Khristov, J. Czarnecki, Effect of bitumen concentration and film thickness on rupture of water-in-oil toluene-diluted bitumen emulsion films using DC polarization, Colloids Surf A Physicochem Eng Asp 519 (2017) 46–59.

[53] Z. Huang, M. Manzo, L. Cai, Machine-learning modeling of asphalt crack treatment effectiveness, Journal of Transportation Engineering, Part B: Pavements. 04021017 (2021).